BRNO UNIVERSITY OF TECHNOLOGY
VYSOKÉ UČENÍ TECHNICKÉ V BRNĚ

FACULTY OF MECHANICAL ENGINEERING
FAKULTA STROJNÍHO INŽENÝRSTVÍ

INSTITUTE OF MATHEMATICS
ÚSTAV MATEMATIKY

MATHEMATICAL MODELLING OF SURFACE WATER WAVES
MATEMATICKÉ MODELOVÁNÍ VLN NA VODNÍ HLADINĚ

MASTER'S THESIS
DIPLOMOVÁ PRÁCE

AUTHOR Bc. Michal Rauš
AUTOR PRÁCE

SUPERVISOR Ing. Tomáš Kisela, Ph.D.
VEDOUCÍ PRÁCE

BRNO 2018

Zadání diplomové práce

Ústav: Ústav matematiky
Student: **Bc. Michal Rauš**
Studijní program: Aplikované vědy v inženýrství
Studijní obor: Matematické inženýrství
Vedoucí práce: **Ing. Tomáš Kisela, Ph.D.**
Akademický rok: 2017/18

Ředitel ústavu Vám v souladu se zákonem č.111/1998 o vysokých školách a se Studijním a zkušebním řádem VUT v Brně určuje následující téma diplomové práce:

Matematické modelování vln na vodní hladině

Stručná charakteristika problematiky úkolu:

Model chování samotné vodní hladiny je nezbytným předpokladem pro simulaci pohybu letounu na vodní hladině. Tato zamýšlená aplikace výsledků určuje základní rámec studovaného problému: hladina chráněna okolním terénem (zátoka), blízko břehu, rychlost větru do 10 km/hod.

Cíle diplomové práce:

Navrhnout a v Matlabu vytvořit model vln na vodní hladině v zátoce blízko břehu. Model zohlední svažování dna, rychlost a směr větru.

Seznam doporučené literatury:

FRANCŮ, Jan. Parciální diferenciální rovnice. 1. Brno: CERM, 2011. ISBN 80-214-4399-0.

KROGSTAD, Harald E. and Øivind A. ARNTSEN. Linear Wave Theory. 1. Trondheim: Norwegian University of Science and Technology, 2000.

Termín odevzdání diplomové práce je stanoven časovým plánem akademického roku 2017/18

V Brně, dne

L. S.

prof. RNDr. Josef Šlapal, CSc. ředitel ústavu	doc. Ing. Jaroslav Katolický, Ph.D. děkan fakulty

Abstrakt
Tato diplomová práce se zabývá matematickým modelováním vodních vln v blízkosti pobřeží pomocí parciálních diferenciálních rovnic. Cílem této práce je formulace pohybových rovnic a jejich následné numerické řešení s grafickou interpretací dosažených výsledků.

Summary
This master's thesis is focused on the mathematical modelling of surface water waves near coasts with the use of partial differential equations. The objective of this thesis is a formulation of equations of motion and their consequent numerical solution with a graphical interpretation of the achieved results.

Klíčová slova
vodní vlny, rovnice mělké vody, metoda konečných objemů

Keywords
water waves, shallow water equations, finite volume method

RAUŠ, M.*Matematické modelování vln na vodní hladině*. Brno: Vysoké učení technické v Brně, Fakulta strojního inženýrství, 2018. 71 s. Vedoucí Ing. Tomáš Kisela, Ph.D.

Rozšířený abstrakt

Tato diplomová práce se zabývá matematickým modelováním vodní hladiny v blízkosti pobřeží při větrných podmínkách a rozličeném tvaru mořského dna. Motivací pro tuto práci je určení bezpečnosti vzletu a přistávání letadel s plovákem na vodní hladině v zátokách při určité rychlosti větru. Rozhodujícimi faktory jsou v tomto případě amplituda a rychlost vln.

Cílem této práce je formulace modelu vodní hladiny, za použití potřebného matematického aparátu, tak, aby tato simulace mohla být následně digitálně implementována v prostředí MATLAB. Zmíněný model by měl zohledňovat právě rychlost větru a tvar dna.

Jelikož požadovaná doména je z hlediska prostoru vícedimenzionální a je třeba vyjádřit řešení také v čase, je nutné využití parciálních diferenciálních rovnic. Nadále je z matematického aparátu rovněž potřebná numerická analýza pro řešení těchto rovnic. Práce využívá nejen matematického základu, ale také elementárních poznatků z hydromechaniky a fluidního inženýrství pro bližší porozumění vzniku a chování vln na hladině.

Práce je strukturována tak, že zpočátku shrnuje vybrané znalosti z teorie parciálních diferenciálních rovnic a numerických metod. Po tomto matematickém aparátu pak následuje seznámení s některými pojmy z fluidního inženýrství, zejména právě popis a chování vln, jelikož tyto charakteristiky je potřeba zvážit při utváření požadovaného modelu.

Následně jsou v práci uvedeny a popsány tři typy rovnic, které byly v průběhu této práce postupně zvažovány jako možné základy modelu a zkoumány. Jmenovitě to jsou Boussinesq rovnice, rovnice mírného sklonu (Mild-slope equation) a rovnice mělké vody (Shallow water equations). Boussinesq rovnice a rovnice mérného sklonu byly postupně v průběhu tvoření práce zavrhnuty, protože jejich složitost přesahovala rámec možností diplomové práce. Tato diplomová práce se tedy především zabývá analýzou a numerickým řešením rovnic mělké vody ve dvou prostorových dimenzích. Pro většinu práce předpokládáme, že dané rovnice jsou homogenní a až v pozdějších kapitolách uvádíme i připojení možných fyzikálních zdrojů do rovnic.

Tyto rovnice byly nejprve odvozeny a následně analyzovány z hlediska vlastních čísel přidruženého kvazi-lineárního systému těchto rovnic. Motivací pro tuto analýzu byl důkaz hyberbolického charakteru těchto rovnic, což bylo následně jedno z důležitých kritérií při výběru vhodné numerické metody pro jejich přibližné řešení.

Při výběru numerické metody pro vytvoření numerického algoritmu, byly zváženy čtyři možné přístupy. Metoda charakteristik, metoda konečných prvků, metoda konečných rozdílů a metoda konečných objemů. Metoda charakteristik byla ihned vyřazena ze seznamu, protože její použití je postaveno na nalezení charakteristik parciální diferenciální rovnice, podél nichž bychom zredukovali problém na systém obyčejných difereniálních rovnic a ty následně řešili numericky některou z metod. Jelikož tato metoda vyžaduje analytické řešení těchto rovnic, které neznáme, byla pro zvažovaný model nepoužitelná. Zbývající tři numerické metody byly všechny možnými variantami. Nakonec byla zvolena metoda konečných objemů z několika důvodů. Zaprvé proto, že kombinuje flexibilitu metody konečných prvků vzhledem ke složitejším geometriím a zároveň jednoduchost metody konečných rozdílů, což je podstatné z hlediska výpočetního času. Nadále je tato metoda často využívána právě pro hyperbolické úlohy, jelikož dobře zvládá nespojitosti, které s sebou i dobře definované hyperbolické problémy přinášejí. Samotná metoda konečných objemů se opírá o princip zákonů zachování určité veličiny, což je příhodné pro rovnice mělké vody, které vycházejí ze zákonů zachování hmoty a momentu.

Jedním z důležitých bodů numerického řešení je generace mrížky, která diskretizuje prostor i čas do dílčích malých objemů. Jelikož jsme v rámci této diplomové práce zvažovali testování numerického řešení na jednoduché a pravidelné geometrii domény, zvolili jsme jako postačující pravidelnou, strukturovanou mřížku. Jsou dva základní přístupy, kde uchovávat informace o přibližném řešení na dílčím objemu během chodu numerického algoritmu. Buď v centru objemu a nebo v uzlech. Pro náš problém jsme zvolili druhou variantu.

V práci následuje odvození numerického schématu založeného na metodě konečných objemů. Jak bylo již zmíněno, při výpočtu stavových proměnných dochází k nespojitostem. Ty vznikají při aproximaci řešení na dílčích objemech diskretizované domény, kdy ve dvou sousedních objemech jsou uchovány dva odlišné stavy proměnných. Když tok prochází přes hranici těchto sousedních objemů, vzniká otázka, jak s touto nespojitostí naložit. Pro tento účel bylo v historii definováno mnoho numerických toků, které tento hraniční tok aproximují a zohledňují oba uložené stavy proměnných.

V této práci jsme zvolili jako numerický tok Rusanův tok, pomocí kterého navrhujeme numerické řešení rovnic mělké vody, v jedné i dvou prostorových dimenzích, s příslušnou CFL podmínkou, nutnou pro stabilitu algoritmu, která slouží pro výpočet velikosti následného časového kroku.

Nadále uvádíme, jak je možné k tomuto numerickému schématu připojit i vliv vnějších zdrojů v případě nehomogenních rovnic mělké vody. To je podstatné pro zahrnutí vlivu větru do rovnic, jak je i požadováno v cílech práce.

V práci následuje obecný popis podmínek, za kterých budeme implementaci v programu MATLAB provádět. Dále je uvedena jedna z možných aproximací vlivu větru na základě jeho rychlosti a konstatního směru vanutí. Počítačová implementace navrženého numerického postupu je pojmenována *SWE2D*. Tento software je přiložen jako součást diplomové práce.

V jeho prostředí bylo otestováno celkem sedm scénářů, ve kterých se postupně měnil počáteční stav hladiny, tvar mořského dna a charakter okrajových podmínek domény. Podmínky větru byly ve všech testovacích případech stejné, jelikož výpočet ukázal, že vliv větru měl oproti tvaru dna zanedbatelný vliv na tvar řešení. Jednotlivé scénáře obsahují motivaci pro jejich zvolení a také nastavené parametry při výpočtu. Grafické výstupy těchto příkladů jsou následně zhodnoceny.

V poslední fázi práce byl proveden jednoduchý test konvergence použitého numerického algoritmu v rámci jednoho z předchozích uvedených scénářů. Spočíval v porovnání posloupnosti přibližných řešení, získaných postupným zjemňováním daného rozměru mřížky, s referenčním řešením. Jelikož přesné řešení rovnic nemáme k dispozici, jako referenční hodnota bylo použito řešení získané pro velmi jemné dělení. Na základě získané posloupnosti relativních chyb jsme konstatovali, že metoda konverguje ke skutečnému řešení.

V závěru jsou navrženy možné nástavby této diplomové práce, které již přesahovaly její rámec. Konkrétně jsou zde uvedeny vnější vlivy, které je možno do numerického schématu zahrnout. Rovněž je zde navrženo užití jiné, přesnější aproximace vlivu větru, jelikož v této práci užitá jednoduchá aproximace nemusí dostatečně přesně popisovat jeho účinek a je nutné porovnání s jinými výsledky pro objektivnější zhodnocení jeho dopadu na řešení. Kromě návrhu na přidání nehomogenních členů do rovnice, je rovněž doporučena formulace metody konečných objemů pro nestrukturované mřížky, které jsou nutné pro popis složitějších a nepravidelných geometrií, kde v této práci použitá strukturovaná mřížka již nestačí. Další možné rozšíření této práce je počítačová implementace za pomocí paralelního a objektového programování pro dosažení lepších výpočetních časů, které jsou při realistických problémech velmi dlouhé.

Cílem této práce bylo navržení a implementace matematického modelu, který by popisoval vodní hladinu v závilosti na tvaru dna a rychlosti větru. Tento cíl byl naplněn, ale je také nutno zdůraznit, že dosažené výsledky jsou spíše prvním krokem pro simulaci realistického modelu, jehož výstupy by šlo nadále využít mimo akademickou půdu. Modelování vodní hladiny je komplexní problém, který musí být řešen pro velmi specifická data a podmínky a i tehdy se nemusí model zdařit. Realistické modelování větrných vln je úloha, která přesahuje náročnost diplomové práce.

I declare, that I wrote my master's thesis *Mathematical Modelling of Surface Water Waves* independently under the guidance of Ing. Tomáš Kisela, Ph.D. using the materials listed in the literature.

Bc. Michal Rauš

I would like to thank my supervisor Ing.Tomáš Kisela, Ph.D. for his thorough and patient guidance.

Bc. Michal Rauš

Contents

1. Introduction

The purpose of this thesis is to propose and also test a mathematical model of water waves in coastal regions. The model should take into the consideration a shape of the ocean bottom and a wind velocity. Since any attempt to even roughly capture the motion of ocean is very complex mathematical task and is usually done for very specific region, this work serves more as an initial stage for such modelling.

The work is based on the application of theoretical knowledge of partial differential equations, numerical methods of solving them and several concepts from hydrodynamics. Although the second chapter serves as a revision of some basic notions used later in the thesis, it's also assumed, that the reader already has some mathematical background.

The structure of the thesis is following:

Chapter 2 introduces the basics from the partial differential equations, numerical analysis and fluid mechanics and is divided into four sections. The first section is dedicated to the review of partial differential equations. The second section introduces some basics from numerical analysis. The third section describes the properties of fluids and classifies the types of flows. The last section is focused on the motion and behaviour of the ocean waves.

Chapter 3 describes three models of the ocean waves, which were considered at different stages of the thesis. The chapter is divided into four sections. The first section describes the Boussinesq equations. The second section introduces the Mild slope equation. The third section is dedicated to the Shallow water equations. In the last section the author of the thesis comments on the chosen model.

Chapter 4 is focused on the analysis of the Shallow water equations and is divided into four sections. In the first section, we derive the Shallow water equations. The second section serves as a summary of forms of the equations. The third section is dedicated to the study of eigenvalues of the set of equations. In the fourth section, we classify the equations with respect to computed eigenvalues.

Chapter 5 describes a numerical solution of the Shallow water equations and is divided into five sections. The first section is dedicated to the choice of numerical method. The second section is focused on the application of finite volume method in one dimensional case of hyperbolic equations. The third section extends this concept into two dimensions. The fourth section proposes a numerical scheme for the numerical solution of the Shallow water equations. The last section introduces the addition of source terms to the numerical algorithm.

Chapter 6 is dedicated to the testing of the program *SWE2D*, created for the purpose of this thesis. It is divided into five sections. The first section describes the model. In the second section, the wind source term is introduced. The third section lists test cases with a graphical representation of the results. The fourth section is a discussion about the achieved results. The fifth section observes the accuracy of the algorithm.

Chapter 7 suggests possible extensions to the work and is divided into two sections. The first section lists numerous source terms, that can be added to the Shallow water equations. In the second section we propose other modifications to the model of ocean waves.

Chapter 8 summarizes and evaluates the thesis.

2. Basic Concepts from Mathematics and Fluid Mechanics

In this chapter, we will briefly look at some basic mathematical definitions and thus familiarize ourselves with mathematical notations, which we will encounter in the following chapters of the thesis. Beside that, we will also describe water properties, several types of ocean waves and some basics from coastal engineering.

The first section is dedicated to the topic of partial differential equations. The second section opens the topic of numerical analysis. The following section is then describing properties of fluids, in our case namely water. The last section introduces the reader to the ocean waves and their behaviour.

2.1. Partial Differential Equations

For this section, dedicated to the partial differential equations, the author has reviewed notes [7] of one of his professors on this subject.

First, we will look at a definition of PDE. Then at the initial and boundary value problems. Lastly, we will classify the PDEs.

Remark. In this section, dedicated to the PDEs, we will use a subscript as a notation for a partial derivative for clarity. However, in the remainder of the thesis, we will use the notation $\frac{\partial}{\partial}$ to avoid any collision with other subscripts.

2.1.1. Definition of PDE

Perhaps the most important concept, which we will use, are *partial differential equations* (also denoted as *PDE*), because this type of equations helps us to describe (at least to some extent) complex physical behaviour around us, e.g. a dissipation of heat in material, a motion of fluids, a weather forecast,... However PDE's can be used in many other branches, for example in finance, civil engineering and even food processing.

By *partial differential equation* we mean an equation, where the unknown is a function of several variables and at least one partial derivative of this function is present in the equation.

For instance, if we consider a function $\eta(x,t)$ of space and time variables $x \in \mathbf{R}$ and $t \in \mathbf{R}^+$, the equation

$$\eta_t = 0, \tag{2.1}$$

where η_t denotes a partial derivative of η with respect to time t, can be considered as a simple case of PDE. The solution of such equation is

$$\eta(x,t) = f(x),$$

where $f(x)$, if there is no other indication, is an arbitrary function of x.

The function η is usually called the *dependent variable* and x, t are called the *independent variables.*

2.1.2. Initial and Boundary Problems

Often in applications, it is not sufficient to only try to solve some partial (or ordinary) differential equation, since they allow for an infinite number of solutions in general. We are more interested in their solution with relation to the physical interpretation and thus we have to also impose some *initial* and *boundary* conditions. These conditions represent the state, from which we want to start the observation and also restrict the solution to the area, where we to examine the equations. Boundary conditions also set the type of the boundaries (it may act like a solid wall, like a free boundary or impose some periodic behaviour on the solution etc...).

A differential equation coupled with an initial condition is called the *initial value problem*. Similarly, by imposing a boundary condition, we obtain the *boundary value problem*. Often both conditions are required at the same time, then we speak of the *initial-boundary value problems*. We impose as many conditions, as needed to obtain an unique solution of the equation. That is a necessary requirement for the problem to be *well posed*.

An example of the initial-boundary problem might be

$$\begin{aligned}
&\text{PDE}: && 4\eta_x + \eta_t = 0 \quad 0 \le x \le L, 0 \le t \le T \\
&\text{IC}: && \eta(x,0) = 0 \quad 0 \le x \le L \\
&\text{BC}: && \eta(0,t) = te^{-t} \quad 0 < t \le T.
\end{aligned}$$

In the literature, we usually encounter these types of boundary condition:

- *Dirichlet* - we specify the value of η on the boundary. For instance

$$\eta(0,t) = \eta(L,t) = 0.$$

- *Neumann* - we prescribe the value of derivatives of the unknown function η on the boundary. For example

$$\eta_x(0,t) = \eta_x(L,t) = 0.$$

- *Robin* - mix of the previous two. An example is

$$\eta(0,t) + \eta_x(0,t) = \eta(L,t) + \eta_x(L,t) = 0.$$

However, when prescribing a boundary condition in our problem, involving the motion of water waves, it will be more beneficial to think of boundaries in terms of their physical interpretation. For that reason, we will consider two types of boundaries - an *outflow* boundary (also a *free* boundary) and a *reflective* boundary. The intuition is quite clear. The free boundary does not effect the passing wave in any way, on the other hand, the reflective boundary changes its direction, which we will achieve by a change of sign in the velocity. But we will specify that later.

2.1.3. Classification of PDE

There are several features, by which we can classify the PDEs.

The first one is by the order of PDE. The *order* of PDE is the order of the highest order derivative present in the equation. For instance the equation (2.1) is of order 1. Another example can be the equation

$$\eta_{xxxx} + \eta_{tt} + \eta = 0,$$

which is of order 4.

Next important differentiating aspect of the PDE is, whether it is linear or not. A PDE is called *linear*, if it is linear in its dependant variable and all its derivatives, with coefficients depending only on the independent variables. If not, then it is called *non-linear*. Some examples:

$$\begin{aligned} \eta_t + c\eta &= 0 \quad c \in \mathbf{R} \\ (x^2 + t^3)\eta_t - c^2\eta_{xx} + \eta &= 0 \\ \eta_t^2 + c\eta_x &= 0 \\ \eta\eta_{xt} - \eta &= 0 \end{aligned}$$

The first two equations are linear, the last two are nonlinear. Most PDEs describing certain phenomenon are fully nonlinear and as such, are difficult or impossible for us to work with. For that reason, we often try to linearize them, usually for a price of significantly reduced accuracy on a large scale.

Let us also define the quasi-linear equations in the case of first order PDEs, since we will encounter this type of equations later in the work. A *quasi-linear* differential equation of first order is an equation of the form

$$\sum_{j=1}^{n} a_j(\boldsymbol{x}, \eta(\boldsymbol{x}))\frac{\partial \eta}{\partial x_j} + b(\boldsymbol{x}, \eta(\boldsymbol{x})) = 0,$$

where $\boldsymbol{x} = (x_1, x_2, ..., x_n)$ and coefficient functions a_j and b are continuous functions.

The third point of view on PDE's classification, is through its homogenity. We say, that a PDE is *homogeneous*, if in the equation doesn't occur any term, which would depend only on the independent variables. In other words, if there isn't a term, which is independent of the unknown function or its derivatives. Otherwise, it is said to be *non-homogeneous*. The equation

$$\eta_{xxx}^3 - \eta_t + 3\eta = 0$$

is homogeneous. The equation

$$\eta_t = 3x$$

is non-homogeneous.

Further we can classify the linear second order PDEs as *hyperbolic*, *elliptic* or *parabolic*. Elliptic equations are often connected with physical problems, which involves a diffusion process, that has reached its equilibrium. For example a temperature distribution at a steady state. The solutions to this type of equations tend to be smooth. Hyperbolic equations, on the other hand, describe a system with discontinuities, like shock waves. Another typical example may be a vibration of a string or a membrane. As for the parabolic equations, the basic example may an one-dimensional heat transfer equation.

In some cases, this classification may be, to a certain extent, be done also in the first-order systems. Let us assume a particular system of the first order quasi-linear equations in the form

$$\frac{\partial \boldsymbol{q}}{\partial t} + \boldsymbol{F}(\boldsymbol{q})' \frac{\partial \boldsymbol{q}}{\partial x} + \boldsymbol{G}(\boldsymbol{q})' \frac{\partial \boldsymbol{q}}{\partial y} = 0, \tag{2.2}$$

where $\boldsymbol{q}$, $\boldsymbol{F}$ and $\boldsymbol{G}$ are some vectors of functions. The notations $\boldsymbol{F'}$ and $\boldsymbol{G'}$ denote the Jacobian matrices of the vectors $\boldsymbol{F}$ and $\boldsymbol{G}$. Then we can classify the system 2.2 as hyperbolic, if its eigenvalues are real and distinct.

2.2. Numerical Analysis

Since we will be unable to solve the governing PDEs analytically, we will need to derive a numerical scheme using some of the known numerical methods in order to solve the equations at least approximately. A numerical solution is often implemented in the engineering applications, not only when an explicit analytical solution cannot be found, but also when finding it would be too "expensive".

2.2.1. Basic Definitions

By the *numerical analysis* we understand the study of approximation techniques for solving approximately mathematical problems, taking into account possible errors.

We call the transformation of a general problem, described by the mathematical equations, into a form, where the inputs and outputs are numbers, a *numerical problem*.

A mathematical tool designed to solve the numerical problem is then a *numerical method*.

The implementation of this method in a programming language is the *numerical algorithm*, we will also use the term *numerical scheme*.

When using some numerical method, we will have to often discretize the area of interest into little elements called *cells* or *elements* or *volumes* and the partition of the domain is called the *mesh* or the *grid*. The grid points are called *nodes*.

When using a numerical algorithm, we want to compute the state of the independent variables at the time t_{n+1}. If the algorithm is such, that it evaluates the state variables at time t_{n+1} only using information at the current time t_n, we speak of *explicit algorithm*. If the algorithm uses an equation with both, the current state of the system at the time t_n and the future one at t_{n+1}, we speak of *implicit algorithm*.

Another important notion is, whether the algorithm is stable or not. The algorithm is *stable*, when the round-off errors of the input data and also of the data obtained during the computation, are not magnified.

2.2.2. Numerical Methods

Usual numerical methods for solving the PDEs are:

- method of characteristics (MOC)
- finite element method (FEM)
- finite difference method (FDM)
- finite volume method (FVM)

Method of Characteristics

This method is based on transforming the PDE into a set of ODEs along the characteristics. The continuous variables in ODEs are transformed into the discrete variables. The discrete equations are then approximations to the continuous ones and are solved by a numerical scheme (like FEM, FVD or FVM).

We have encountered this approach being used in the modelling of blood flow. The use of MOC is lmited in general, however. That is due to the fact, that many problems don't have an analytical solution and therefore we are unable to find characteristics, which is the basis of this method.

Finite Element Method

The idea of FEM is to discretize the domain, where we want to solve the PDE, into elements, which are connected at nodes. Each finite element is a part of the domain, over which are the unknown variables defined by the equations of the considered problem. Over each of these elements, the solution of the equations is approximated by basis functions, which interpolate the unknown variables over the element. The basis function are defined within each element using the values of the variables at nodes. The approximate solution to the equations over the element is given by a linear combination of the values of the variables at nodes and the basis functions. The initial and boundary conditions have to be applied to the elements in order to obtain an approximated solution. At the end, the local approximations are assembled together.

The main advantage of FEM is the ability to handle a very complex geometry of the domain. FEM is also convenient when the problem has complex restraints. For these reasons, FEM is used in a variety of engineering problems concerning solid and fluid mechanics, heating models and electrostatic problems.

The disadvantage, on the other hand, is the needed number of nodes. Specifically, as we want to obtain a more accurate result, we need to increase the number of nodes, which means increased number of points for solution. The result is an increased computational time.

Finite Difference Method

This is one of the oldest and simplest methods used to solve differential equations. Even Euler (18. century) was aware of it. With the advancement of computational technologies, this method became very popular around 1950s and is still used to this day.

The basic idea is again a partition of the domain in time and space and obtain a mesh. Then we approximate the continuous derivatives in the equation by Taylor expansions around the nodes, where all the obtained equations and variables are stored. At last, we solve all the equations, using the data from the initial and boundary conditions, for a given time step. This solutions are again used for another time step and so on.

The advantage of FDM is the easy implementation of the method, which is the reason for its often application in the engineering problems.

On the other hand, the offset of this method is, that it is not flexible enough for more complex or irregular boundaries.

Finite Volume Method

The finite volume method originated sometimes around the mid-fifties of the last century and since then, have became one of the most used tools in the computational fluid mechanics.

The idea of FVM is partitioning the domain into small finite volumes (thus the name of the method). This method is based on the conservation nature of many physical laws, which means, what enters the cell must also leave the same cell on the other side. In each cell, the integral equations are applied to obtain the specific conservation within the cell. This is one of the reasons, why FVM is so often used in hydrodynamics problems, where the equations of flow are based on the conservation of mass and momentum.

There are typically two used ways for storing the information (the initial and boundary conditions, the approximated solutions and values of variables) with respect to the generated mesh - *node-centered* and *cell-centered*. It cannot be said, that one is universally better (more efficient) than the other, it depends case by case and both are commonly used. These approaches are depicted in the fig. 2.1.

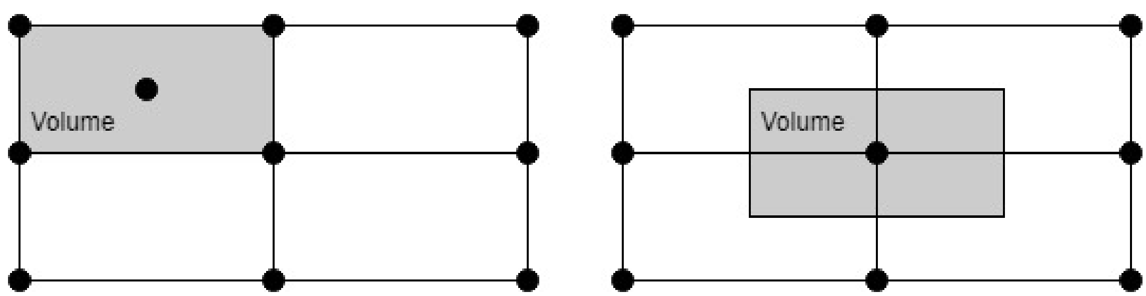

Figure 2.1: *The cell-centered approach on the left and the node-centered on the right.*

The finite volume method is a very popular, because it is seen as the ”best of both worlds” option, since it is similar in its simplicity to FDM, but possesses the geometrical flexibility of FEM. Also FVM doesn’t require a coordinate transformation when using irregular meshes, but can be applied to them right away.

2.2.3. Riemann Problem

One of the features of FVM is, that there discontinuities in state variables between two cells. The Riemann problem describes the situation of a breakup between two constant states. Let us assume a simple one-dimensional linear case of Riemann problem to illustrate a discontinuity in a hyperbolic system. The initial value problem is then

$$q_t + aq_x = 0$$
$$q(x,0) = q_0(x) = \begin{cases} q_L & if\ x \leq 0 \\ q_R & if\ x > 0 \end{cases}$$

The states u_L and u_R are constant and a is a positive characteristic speed. Many problems involving discontinuities solve the Riemann problem and then use the information to compute the numerical flux. The linear problems are solved by computing eigenvectors and eigenvalues. In general case, an approximate Riemann solvers have been developed.

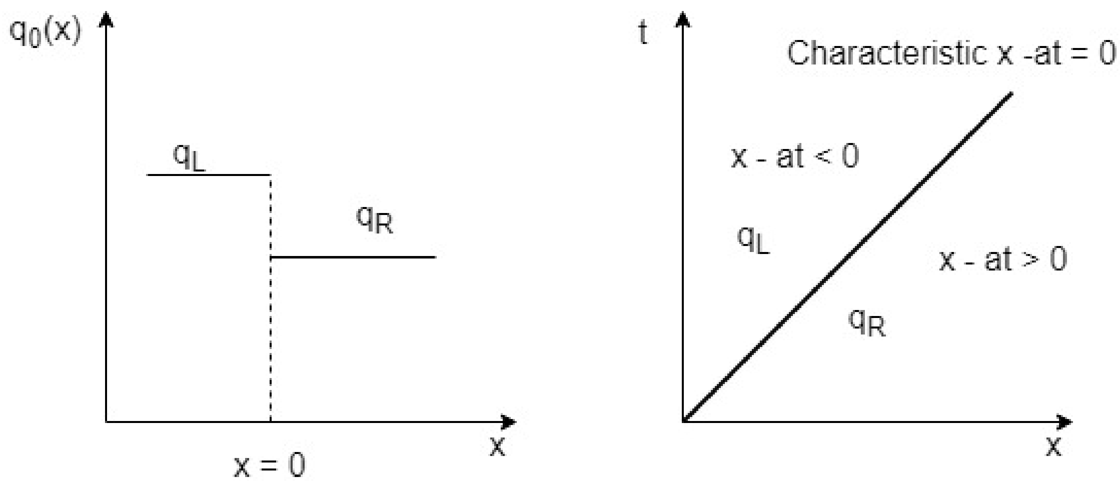

Figure 2.2: *On the left the illustration of initial data. On the right a solution to the linear problem.*

Roe's Solver

Roe proposed (1981) an approximate solution to the Riemann problem and since then, this solver is widely used. The idea is to approximate the non-linear system of conservation laws by a linearized system with constant coefficients, but with the same initial data as for the exact problem.

In general, the equations in the Riemann problem can be non-linear

$$\frac{\partial \boldsymbol{q}}{\partial t} + \frac{\partial \boldsymbol{F}(\boldsymbol{q})}{\partial x} = 0. \tag{2.3}$$

We denote by A the Jacobian matrix of $\boldsymbol{F}(\boldsymbol{q})$. Then

$$A = \frac{\partial \boldsymbol{F}}{\partial \boldsymbol{q}}.$$

Therefore we can write (2.3) as a linearized system

$$\frac{\partial \boldsymbol{q}}{\partial t} + A\frac{\partial \boldsymbol{q}}{\partial x} = 0. \tag{2.4}$$

Roe's idea was to replace the Jacobian matrix A in (2.4) by a constant Jacobian matrix

$$\tilde{A} = \tilde{A}(\boldsymbol{q}_L, \boldsymbol{q}_R),$$

which is a function of the data states $\boldsymbol{q}_L, \boldsymbol{q}_R$. This way the equation (2.4) is replaced by a linear system with constant coefficients

$$\frac{\partial \boldsymbol{q}}{\partial t} + \tilde{A}\frac{\partial \boldsymbol{q}}{\partial x} = 0.$$

2.2.4. Courant-Friedrichs-Lewy Condition

The *Courant-Friedrichs-Lewy condition*, or also the *CFL condition*, is a necessary condition for ensuring, that the numerical algorithm is stable. It is used to compute the next time step size in an algorithm.

If we considered a one-dimensional case

$$\frac{\partial \boldsymbol{q}}{\partial t} + \frac{\partial \boldsymbol{F}(\boldsymbol{q})}{\partial x} = 0,$$

where the numerical algorithm computes the state of variables after a time step Δt in an element of length Δx, the CFL condition would be

$$\frac{\lambda_{F,max}\Delta t}{\Delta x} \leq C_{CFL}, \tag{2.5}$$

where $\lambda_{F,max}$ is the maximum absolute value for eigenvalues of the Jacobian matrix $\boldsymbol{F}(\boldsymbol{q})'$. The choice of C_{CFL} depends on the problem, but generally $0 < C_{CFL} \leq 1$.

For the two-dimensional case

$$\frac{\partial \boldsymbol{q}}{\partial t} + \frac{\partial \boldsymbol{F}(\boldsymbol{q})}{\partial x} + \frac{\partial \boldsymbol{G}(\boldsymbol{q})}{\partial y} = 0$$

is the condition similarly in form

$$\frac{\lambda_{F,max}\Delta t}{\Delta x} + \frac{\lambda_{G,max}\Delta t}{\Delta y} \leq C_{CFL}, \tag{2.6}$$

where the cell is $\Delta x \times \Delta y$ and $\lambda_{G,max}$ is the maximum absolute value for eigenvalues of the Jacobian matrix $\boldsymbol{G}(\boldsymbol{q})'$.

2.3. Properties of Fluids and Types of Flows

The purpose of this section is to introduce the reader to some selected properties of fluids and types of their flows, since these facts have to be taken into account, when we are considering a model of coastal waves. For further study of fluid properties, it is recommended to read these books [4, 8], which are also sources for this section of the thesis.

The first part of this section is dedicated to the definition of the no-slip condition. The second subsection introduces the density and the corresponding classification of compressible and incompressible flows. The following subsection is focused on the viscosity of fluids and differentiate between the viscous and non-viscous flows. The fourth part of this section explains the difference between the laminar and turbulent flows. The fifth subsection similarly divides flows into rotational and irrotational. The sixth subsection defines steady and uniform flows. The last part of this section explains the meaning of the dimension of a flow.

In general the term *fluid* includes both gas and liquid phases of a substance. The distinction between liquids and gases then lies in a molecular spacing, intermolecular forces, a movement of molecules and a shape of the substance in a container. Although we will be addressing the properties of fluids in general in this section, we are interested in the properties of water in particular.

2.3.1. No-Slip Condition

Although it might be more suitable to discuss this condition of flows in later stages of the thesis, we will refer ourselves to it already in this section. For that reason, we will present it here.

Since a fluid flow is often confined by solid objects, it is important to know, how do the solids and fluids interact. Although we know even from an observation, that fluids can't go through solid objects (considering objects impermeable to a fluid) and stop at the surface, what happens, when a fluid comes at an angle to a solid obstacle?

The *no-slip condition* states, that when a fluid comes to a contact with a solid surface, it "sticks" to it due to viscous forces, so there is no "slip". This means, the fluid will stop and assume zero velocity, relative to the solid surface. If the solid object is not moving, the layer of the fluid in contact with the surface comes to stop as well.

The no-slip condition is responsible for the development of a velocity profile of a flow. The layer of fluid adjacent to the solid surface will slow down neighboring layer of the fluid. This layer will slow down another one and so on.

2.3.2. Density

The *density* of a substance is defined as its mass per unit volume and is usually denoted by the symbol ρ and its SI unit is $[kgm^{-3}]$. The density in general is not constant for an object, since it's dependent on a pressure and a temperature. For instance higher pressure on the object will decrease its volume and thus increase its density. Therefore different parts of an object may differ in density with progressing time. This may not be so notable for solids, but it is for fluids.

We determine the fluid density at given point by enveloping this element by a small volume of fluid ΔV. The corresponding mass of the fluid in this volume is Δm. The density of the element is then

$$\rho = \lim_{\Delta V \to 0} \frac{\Delta m}{\Delta V}.$$

However, usually we just consider an average density of an object of mass m and volume V or assume, it is uniformly dense and thus compute its density

$$\rho = \frac{m}{V}.$$

Based on the variation of fluid density, we can classify its flow as either *compressible* or *incompressible*. By an incompressible flow we mean, that the density of the fluid is nearly constant. This means, that the volume of every portion of fluid remains constant during its motion.

Although no fluid in real life is perfectly incompressible, we assume it in most cases to simplify the calculations. For instance, we can take the *continuity equation* in the differential form describing the conservation of mass

$$\frac{\partial \rho}{\partial t} + \nabla \cdot (\rho \boldsymbol{u}) = 0,$$

where ρ is the density and $\boldsymbol{u}$ is the fluid velocity. This equation is valid for compressible fluids. If we assumed an incompressible flow, it would mean, that

$$\frac{\partial \rho}{\partial t} = 0$$

and ρ could be also taken out of the divergence operator, because now the density is not a function of time and space. Thus leaving us with the continuity equation for incompressible flows in the form

$$\nabla \cdot \boldsymbol{u} = 0. \tag{2.7}$$

Liquids are usually considered incompressible, since there is a little variation in density with a change of conditions. For example, if we consider a water under the pressure of 1 *atm* and 210 *atm*, the difference in density is only 1 percent. The same however doesn't hold true for gases, which are generally considered compressible fluids.

2.3.3. Viscosity

Viscosity is a measure of a fluid resistance to flow. Perhaps a better approach to describe viscosity is an intuitive one with an example.

Let us assume, we have two solid objects sharing a contact surface - a book lying on a table. If we try to move the book, a friction force will act on it as well in the opposite direction of the movement. We would have to overcome this friction by force in order to move the book. The magnitude of the required force would be dependant on a friction coefficient between the book and the table. Something similar occurs, when two fluids or a fluid and a solid come to contact. For instance a tablespoon sinks much faster in a glass of water than into a jar full of honey.

Viscosity describes a fluid internal resistance to deformation. It's due to internal friction forces, which develop between different layers of a fluid, which move relative to each other. A fluid with lower viscosity flows more easily and vice-versa.

In order to capture the viscosity in more concrete terms, let us consider an idealized situation known as the Couette flow (fig. 2.3). In this case, we have two very large parallel plates (so large, we do not have to consider the edges) and a fluid between them. The distance between the plates is l. If we apply a constant parallel force F on the upper plate, it will start moving and after a while, it will move with a constant speed U.

The layer of fluid in contact with the upper plate will move at the same speed as well (see 2.3.1) and the shear stress acting on it is then

$$\tau = \frac{F}{A},$$

where A is the area of the contact surface between the plate and the fluid. On the other hand, the bottom layer of the fluid in contact with the bottom stationary plate will

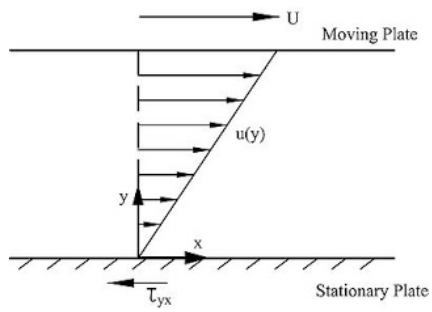

Figure 2.3: *Couette flow.* Image downloaded from
https://sites.google.com/site/arifosu/resource/2d-couette-flow–simple-algorithm

move with zero velocity (again 2.3.1). In case of a steady laminar flow, the fluid velocity will vary linearly between the two plates, so the profile of the fluid velocity is

$$u(y) = \frac{y}{l}U, \tag{2.8}$$

where y is the vertical distance measured from the bottom plate. If we differentiate (2.8) with respect to y, we get the gradient of fluid velocity

$$\frac{du}{dy} = \frac{U}{l}. \tag{2.9}$$

It can be experimentally concluded, that for most fluids, the rate of deformation and thus the velocity gradient, is proportional to the shear stress τ

$$\tau \propto \frac{du}{dy}. \tag{2.10}$$

If the two are linearly proportional, we speak of a *Newtonian fluid.* For example water and air are both commonly considered to be Newtonian fluids, honey and blood are not.

In case of Newtonian fluids, the relationship (2.10) is expressed by

$$\tau = \mu\frac{du}{dy}, \tag{2.11}$$

where μ is called the *dynamic viscosity.* Its SI unit is $[kg\, m^{-1}s^{-1}]$.

The shear force acting on a fluid layer is

$$F = \tau A = \mu A\frac{du}{dy} = \mu A\frac{U}{l},$$

if we recall (2.9) and (2.11).

The dynamic viscosity of a fluid is measured experimentally from this expression by recreating conditions similar to those of the ideal Couette flow, when the applied force F, the area of contact A, the velocity of a moving plate U and the distance of the plates l are known.

Besides the dynamic viscosity there is also a *kinematic viscosity.* It's usually denoted by ν with SI unit $[m^2s^{-1}]$ and can be computed

$$\nu = \frac{\mu}{\rho},$$

where ρ is a density.

The viscosity of a fluid is dependent on a temperature (also on a pressure, but that is not so significant). The kinematic viscosity of fluids decreases with increasing temperature, however the kinematic viscosity of gases increases with increasing temperature.

Based on a viscosity of a fluid, we can differentiate between *viscous* and *non-viscous* flow. In the non-viscous flow, the internal friction is neglected and thus there are no viscous forces. The flow then flows without an energy loss. Non-viscous flow does not necessarily mean that the viscosity of the fluid is considered to be zero, but rather that the viscous forces vanish.

A water has dynamic viscosity $\mu = 0.0010$ at 20°C and $\mu = 0.0018$ at 0°C. For solving numerous hydrodynamics problems, it is often considered to be zero. Although neglecting such relatively low viscosity may be acceptable for certain situations, it it still important when considering a contact of a fluid with a solid object.

2.3.4. Laminar and Turbulent Flows

In this part of the thesis, we will look at laminar and turbulent types of flows. First let us consider a flow in a pipe, which holds a little importance for coastal problems, but still provides some insight and then we describe flows in channels, which are closer to our geometry.

Intuitively, we could say, that a flow being laminar or turbulent means, how "orderly" the flow behaves (fig. 2.4). Laminar flow describes a situation, when the fluid particles move in adjacent parallel layers of the fluid (*laminates*) in the same direction without disruption between the layers. This kind of behaviour can be observed for fluids with a high viscosity and flowing at a low speed. For instance air flowing around a wing of an aircraft can be considered a laminar flow. On the other hand a turbulent flow displays much more chaotic behaviour and velocity fluctuations. Such is usually the case of low-viscous fluids moving at higher velocities.

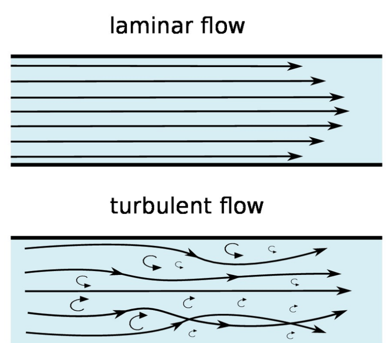

Figure 2.4: *Laminar and turbulent flows.*. Image downloaded from https://www.cfdsupport.com/OpenFOAM-Training-by-CFD-Support/node275.html

A transition from one state to the other is not immediate, but there is also a regime in between called *transitional*.

If we consider a flow of a fluid in a pipe, we can observe, that at low velocities, the flow is laminar, however once the velocity crosses a critical value, the flow becomes turbulent. The transition between the two is best described by the Reynold's number

$$Re = \frac{\rho V_{avg} D}{\mu},$$

where V_{avg} is average flow velocity, D characteristic length of the geometry (in case of a pipe its diameter), ρ density and μ dynamic viscosity. Reynold's number is a dimensionless quantity.

For each flow is computed a critical value of the Reynold's number, which is influenced by the flow conditions and geometry. If the Reynold's number of the current state of the flow is below this threshold, then the flow is considered to be *laminar*. If it's greater than the critical value, then the flow is *turbulent*. If it is close to the critical value, then a transitional regime is assumed. In such case the flow can randomly jump between being laminar and turbulent. A laminar flow is viable even after surpassing the critical value of Reynold's number, if the pipes are sufficiently smooth and pipe's vibrations are avoided.

Now let us consider a flow in an *open channel*. That mean a channel open to the atmosphere or partially filled conduits. An open channel is characterized by the presence of a liquid-gas interface called the *free surface*. Examples of an open channel may be a river, a drain or a sewer.

In an open channel, the fluid velocity is zero at the bottom and on the sides due to the *no-slip condition* (see 2.3.1) and is maximum in the middle of the channel near the free surface. The velocity varies not only in the cross section, but also along the channel, making the distribution of the fluid velocity three-dimensional. However, just an averaged velocity for the cross section of the channel is usually considered for the engineering problems, making the problem only one-dimensional.

Similarly to the flow in pipes, the flow can be laminar, transitional and turbulent. The classification again depends on the values of Reynold's number given by

$$Re = \frac{\rho V_{avg} D_H}{\mu},$$

where D_H is a *hydraulic diameter*, defined as

$$D_H = \frac{A_c}{p}.$$

A_c is the cross-sectional flow area and p is the *wetted perimeter*. A wetted perimeter is the total linear distance in a cross section of a channel, that is in contact with water. For fully closed circular channel (a pipe), D_H would reduce to just a radius.

Laminar regime of a flow is preferred for solving problems, however most kinds of flows (especially in nature) are turbulent. They can display laminar type of behaviour only, when the flow is very close to a solid object. Modelling a turbulent flow is very challenging, because of

- unsteady and aperiodic motion of the fluid
- fluid properties exhibit random spatial variations, which leads to 3-D problems
- there is a strong dependence on initial conditions
- the flow contains *eddies* (fluid current, whose flow direction differs from the general flow)

This means, that a simulation of a turbulent flow must be three-dimensional, time accurate and based on a fine grid.

2.3.5. Rotational and Irrotational Flows

To differentiate between a rotational and an irrotational flow, we will need to introduce a *vorticity vector*

$$\boldsymbol{\xi} = \nabla \times \boldsymbol{u},$$

where $\boldsymbol{u}$ is the velocity vector of a fluid.

If the vorticity $\boldsymbol{\xi}$ is non-zero at certain point of a flow field, the fluid particle which happens to occupy that point of space is rotating and the flow in that region is called *rotational.* If the vorticity is zero (or sufficiently close) at certain area, the particles there don't rotate and the flow is called *irrotational* there. Usually regions near solid boundaries are rotational and fluid particles outside the viscous boundary layer are irrotational.

The vorticity of fluid particles can be changed only through an external action, otherwise the nature of a flow remains the same. Thus if a flow originates from an irrotational area, it will remain irrotational, until some process alters it.

In real-life situations flows are rotational, we just assume they are irrotational in order to be able to solve the corresponding problem. The simplification in fluid mechanics is based on the vector identity concerning the curl of the gradient of any (however sufficiently smooth) scalar function ϕ. This identity states, that

$$\nabla \times \nabla\phi = 0,$$

which applies to any orthogonal coordinate system. This means, that if

$$\nabla \times \boldsymbol{u} = 0$$

for some vector $\boldsymbol{u}$, then

$$\boldsymbol{u} = \nabla\phi. \tag{2.12}$$

In words, if the curl of a vector is zero, then the vector can be expressed as the gradient of a scalar function ϕ, which is called the *potential function.* In fluid mechanics $\boldsymbol{u}$ is the velocity field, its curl is the vorticity $\boldsymbol{\xi}$ and ϕ is the velocity potential function. If we assume the continuity equation (2.7) for incompressible flows

$$\nabla \cdot \boldsymbol{u} = 0$$

and take into consideration (2.12), we get for the irrotational regions of the flow

$$\nabla \cdot \boldsymbol{u} = \nabla \cdot \nabla\phi = \nabla^2\phi = 0, \tag{2.13}$$

which is called the *Laplace equation*, where ∇^2 is the *Laplacian operator*.

Similarly, let us consider the *Navier-Stokes equation*, valid for incompressible flow of a Newtonian fluid with constant properties,

$$\rho\left[\frac{\partial \boldsymbol{u}}{\partial t} + (\boldsymbol{u} \cdot \nabla)\boldsymbol{u}\right] = -\nabla p + \rho\boldsymbol{g} + \mu\nabla^2\boldsymbol{u},$$

where ρ is the density, p is the fluid's pressure, $\boldsymbol{g}$ the gravitational acceleration and μ the dynamic viscosity. By assuming an irrotational flow and thus taking into the account (2.13), we can completely drop the last viscous term on the right hand side of the equation and by doing so, simplify the model, since

$$\mu\nabla^2\boldsymbol{u} = \mu\nabla^2\nabla\phi = \mu\nabla(\nabla^2\phi) = 0.$$

2.3.6. Steady and Uniform Flows

This short section deals with the distinction between these two types of flows.

Steady means, that there is no change at a point with time. Meaning, if we have a steady flow, the fluid particles properties can change with position, but at any fixed point they remain constant with time e.g. the mass, the volume, the total energy... Any flow, that is not steady, is *unsteady.*

Uniform means, that there is no change with location. The fluid particles properties can vary with time, but at any given time, they have to be constant along the whole flow.

2.3.7. Dimension of a Flow

The dimension of a flow is usually connected to the dimension of the fluid velocity field. Thus the flow is said to be *one-*, *two-* or *three-dimensional*, if the velocity varies in one, two, or three primary dimensions.

Although most problems involve three-dimensional flows, the dimension can be reduced, if the velocity variance in certain direction is assumed to be negligible or small relative to the variance of the velocity in other directions. Whether such assumption is valid or not depends on the situation, but it is an often sought option, since it simplifies the problem considerably.

2.4. Ocean Waves

This section will introduce some basics of the ocean waves.

The first subsection provides a description of the ocean waves. The second part of this section then deals with the classification of the ocean waves. The third subsection is focused on the linear wave theory. The fourth subsection describes a generation of wind waves. The last part of this section examines the behaviour of the waves.

2.4.1. Description of Ocean Waves

Waves on a water's surface are a common observation. These waves are caused by an energy passing through the water, which creates a circular motion of the water particles. The waves originate from a point of energy disturbance and without obstacles, can travel across the whole ocean. Waves transport energy, not matter.

Now let us provide a brief description of the ocean waves.

crest - the local maximum of the shape of a wave

trough - the local minimum of the shape of a wave

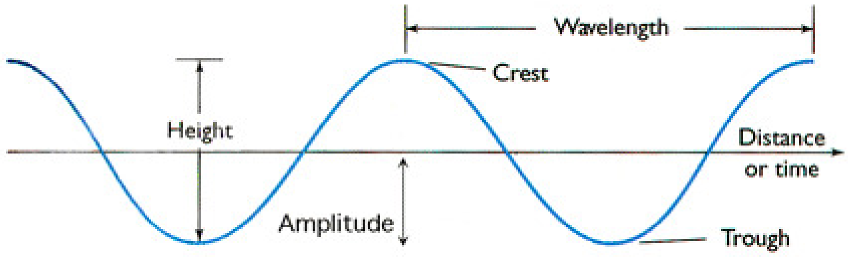

Figure 2.5: *Wave characteristics.* Image downloaded from https://www.eoas.ubc.ca/courses/atsc113/sailing/met_concepts/08-met-waves/8b-wave-characteristics/index.html

wave height H $[m]$ - the difference in height between the crest and the trough of a wave

amplitude a $[m]$ - a half of the height of a wave

wavelength L $[m]$ - the horizontal distance between two neighbouring crests

wave period T $[s]$ - the time for one full wavelength to pass a given point

wave steepness [-] - the ratio of the wave height to the wavelength

mean sea level - an average level of the surface of the ocean

depth d $[m]$ - the vertical distance between the sea bed and the mean sea level (surface of the sea at rest)

phase velocity c $[ms^{-1}]$ - the ratio of the wavelength to the period

wave number k $[m^{-1}]$ or $[rad\, m^{-1}]$- the number of wavelengths per distance unit

2.4.2. Classification of Ocean Waves

The ocean waves can be classified by several factors, but for our purposes it will suffice to differentiate between them by examining the disturbing and restoring forces. By disturbing forces, we mean forces, which cause the creation of a wave and restoring forces are such, that destroy the wave. In this section we will also introduce important notions of shallow water waves and deep water waves.

wind waves - these waves arise by the effect of a blowing wind. There are three types of wind waves:

capillary waves - these waves are distinguished by a short wavelength and a short wave period. They arise by the effect of a wind, blowing at low speeds and they vanish thanks to a surface tension.

gravitational waves - these waves are the next stage of the capillary waves. They are also generated by the wind, however as the wave height increases due to higher speeds of the wind, these waves overcome the surface tension. They can be meters to kilometres long. The restoring force in this case is the gravity, which drags the waves down. These waves are probably the most common ones, when it comes to modelling of ocean waves. This thesis is also build around them.

swells - these waves are gravitational waves, but rather than being generated by a local wind, they are generated by distant storms and heavy winds. They are capable of travelling long distances across the ocean with a little loss of energy. Swells with larger wavelengths usually have lower wave heights, however also carry more energy and thus can form into dangerous breaking waves near shore.

tsunamis - these waves are characterized by very long wave lengths (even more than 200 km), high speeds (can be higher than 700 km/h) and high amplitudes. The waves can appear small at open sea, however as they reach a coast and thus shallower waters, they slow down and the amplitude starts to rise rapidly. The disturbing force is a seismic activity (e.g. a sudden movement of earth's crust, an earthquake, a volcanic activity, an explosion...). The restoring force is again the gravity. These waves have devastating effect on the infrastructure, therefore there exist numerous prediction models.

tidal waves - these waves have large both wave lengths and period. The are caused by the effect of gravitational interactions of Earth, Sun and Moon and also by the rotation of Earth. The restoring force is the Earth's gravity.

storm surges - they are generated by low pressure systems like hurricanes. Because of the low pressure, these waves can be larger than the wind generated ones. They are destructive in low-lying areas.

standing waves - these waves sometimes arise as a result of a wave interference.

others - there are more types of waves, but the listed ones here are probably those mainly discussed. Others may include rogue waves, waves caused by a passing ship or some other machinery etc....

Another important distinction between the types of waves is, whether we speak of *shallow water, deep water* or *intermediate depth waves.* Suppose, d is the sea depth at some area, L is the wavelength and k is the wave number of the wave passing this region. According to [18], we can define the mentioned terms as follows:

Range of kd	Range of d/L	Type of wave
0 to $\pi/10$	0 to 1/20	*Shallow water waves*
$\pi/10$ to π	1/20 to 1/2	*Intermediate depth waves*
π to ∞	1/2 to ∞	*Deep water waves*

Sometimes in the literature, instead of using the term shallow water waves, the author speaks only of the *shallow water* and analogically for the deep water waves.

Although this separation of the sea on being shallow and deep based on the wavelength of a passing wave might not be intuitive, it will make much more sense once we discuss the motion of waves (2.4.3).

2.4.3. Linear Wave Theory

Since any attempt to capture the motion of the ocean is a very difficult task, up to this day, we still rely on the Airy linear wave theory (1845). Although this theory requires quite heavy restrictions and is only a simplification of the real-life problem, it is still studied and applied, because of its capability to produce a tractable solution. Foremost, it allows us to have at least some understanding of the motion of the waves.

In the thesis, we will provide just basics of the linear wave theory. For more details, we kindly refer the reader to [18], where the topic is explained very nicely and much more thoroughly. This book is also one of the main sources for this part of the thesis along with [15].

Remark. In this subsection concerning the Linear wave theory, we will keep the notation η as a function of the free surface, however, it will be measured from the mean sea level (sea surface at rest). We will encounter this notation later in the thesis, when we will discuss the Shallow water equations more thoroughly, but then the reference plane will be a bit different and specified accordingly.

Assumptions

These simplifying assumptions are made in order to obtain a sensible solution:

- The water has a constant depth d and a constant wavelength L (or period T)
- The water motion is two-dimensional (thus a constant height along the crests)
- The form of waves is constant, they do not change with time
- The water is incompressible
- The effects of viscosity, turbulence and surface tension are neglected
- The wave height H is small compared to the wavelength L and the water depth d (i.e. $H/L \ll 1$ and $H/d \ll 1$)

Conservation of Mass and Momentum

Considering the listed assumptions, the governing equations will represent the conservation of mass and momentum. The conservation of mass is given by the Laplace equation (see 2.13)

$$\frac{\partial^2 \phi}{\partial x^2} + \frac{\partial^2 \phi}{\partial z^2} = 0, \tag{2.14}$$

where ϕ is the velocity potential, x represents the horizontal position and z the vertical one.

The velocity potential is defined by the horizontal u and vertical w components of the velocity

$$u(x, z, t) = -\frac{\partial \phi}{\partial x} \tag{2.15}$$

$$w(x,z,t) = -\frac{\partial \phi}{\partial z}. \tag{2.16}$$

The conservation of momentum is represented by the unsteady Bernoulli equation

$$-\frac{\partial \phi}{\partial t} + \frac{p}{\rho} + gz = 0, \tag{2.17}$$

where p is the pressure, ρ is the density and g is the gravitational acceleration.

Boundary Conditions

(i) Dynamic boundary condition for the free surface:
At the free surface η, the pressure is atmospheric, thus $p = 0$. For that reason (2.17) simplifies to

$$-\frac{\partial \phi}{\partial t} + g\eta = 0 \quad at \quad z = 0. \tag{2.18}$$

More accurately, the condition should be at $z = \eta$, however because of the requirement for small amplitudes (the last assumption in (2.4.3)), we can take $\eta \to 0$.
(ii) Kinematic boundary condition at the free surface:
This condition states, that at the free surface, there can be no transport of fluid through it (since the free surface defines the shape of the ocean surface). Mathematically this is captured by putting the vertical velocity of the fluid equal to the vertical velocity of the free surface.

$$w = \frac{D\eta(x,t)}{Dt} = \frac{\partial \eta}{\partial t} + u\frac{\partial \eta}{\partial x} \quad at \quad z = \eta \tag{2.19}$$

The right hand side of the condition represents the vertical velocity of the free surface.
Now we substitute (2.16) into (2.19) and use again the assumption of small amplitudes. This means, that $\frac{\partial \eta}{\partial x} \to 0$, because the amplitude will not vary much along the horizontal axis. Thus we get

$$-\frac{\partial \phi}{\partial z} = \frac{\partial \eta}{\partial t} \quad at \quad z = 0. \tag{2.20}$$

(iii) Kinematic boundary condition at the sea bed:
This condition is similar to the one for the free surface, except now we require, that the fluid can't go through the sea bed.

$$w = -\frac{\partial \phi}{\partial z} = 0 \quad at \quad z = -d \tag{2.21}$$

Solution

Now, we would have to solve the equation (2.14) with the boundary conditions (2.18), (2.20) and (2.21). Airy solved it using the separation of variables and obtained the following result

$$\phi(x,z,t) = \frac{ag}{\omega}\frac{cosh[k(d+z)]}{cosh(kd)}cos(kx - \omega t), \tag{2.22}$$

where a is the amplitude, $\omega = 2\pi/T$ is the angular velocity and $k = 2\pi/L$ is the wave number.

Wave Profile

We can rearrange the dynamic boundary condition (2.18) to get

$$\eta = \frac{1}{g}\frac{\partial\phi}{\partial t} \quad at \quad z = 0. \tag{2.23}$$

By substituting (2.22) into (2.23) and computing the derivative with respect to t, we would obtain

$$\eta = a\, sin(kx - \omega t). \tag{2.24}$$

From this we learn, that in linear theory, the waves propagate in sinusoidal manner.

Dispersion Relationship

By substituting (2.23) into the kinematic boundary condition at the free surface (2.20) and computing the derivative, we get

$$-\frac{\partial\phi}{\partial z} = \frac{1}{g}\frac{\partial^2\phi}{\partial t^2} \quad at \quad z = 0. \tag{2.25}$$

Then by using the result for the velocity potential (2.22) in (2.25), considering $z = 0$ we would obtain

$$\omega^2 = gk\, tanh(kd). \tag{2.26}$$

The expression (2.26) is called the *dispersion relationship*. It puts into a relationship the angular velocity ω, the wave number k and the depth d.

Phase Speed

By definition (2.4.1), the phase velocity c is computed

$$c = \frac{L}{T}$$

or equivalently

$$c = \frac{\omega}{k}. \tag{2.27}$$

Substituting the dispersion relationship (2.26) into (2.27) yields

$$c^2 = \frac{g}{k}\, tanh(kd). \tag{2.28}$$

The phase speed defined in (2.28) is also called the *celerity*.

Motion of Water Particles

By substituting (2.22) into the definitions of the horizontal (2.15) and the vertical (2.16)) components of the velocity, one obtains

$$u = \frac{agk}{\omega} \frac{cosh[k(d+z)]}{cosh(kd)} sin(kx - \omega t) \tag{2.29}$$

$$w = -\frac{agk}{\omega} \frac{sinh[k(d+z)]}{cosh(kd)} cos(kx - \omega t). \tag{2.30}$$

The horizontal ξ and vertical ζ displacements (measured from the mean sea level) of the water particle can be expressed as

$$\xi = \int u\, dt \quad and \quad \zeta = \int w\, dt. \tag{2.31}$$

For this definition the reader can recall the physics lessons, where the time derivative of a particle's position was computed to obtain its velocity at the point.

By combining the expressions (2.29), (2.30) and (2.31) and integrating, we would get

$$\xi = \frac{agk}{\omega^2} \frac{cosh[k(d+z)]}{cosh(kd)} cos(kx - \omega t) \tag{2.32}$$

$$\zeta = \frac{agk}{\omega^2} \frac{sinh[k(d+z)]}{cosh(kd)} sin(kx - \omega t). \tag{2.33}$$

By substituting the dispersion relationship (2.26) into (2.32) and (2.33), these expression can be rearranged to obtain

$$\frac{\xi^2}{A^2} + \frac{\zeta^2}{B^2} = 1, \tag{2.34}$$

where

$$A = a\,\frac{cosh[k(d+z)]}{sinh(kd)}$$

$$B = a\,\frac{sinh[k(d+z)]}{sinh(kd)}.$$

Discussion of the Linear Wave Theory

In this last part of the linear wave theory section, we will comment some of the results presented above. For that purpose, it would be beneficial to notice, what are the approximate values of the functions $sinh(kd)$, $cosh(kd)$ and $tanh(kd)$ in limit cases, when $kd \to 0$ and $kd \to \infty$.

	$kd \to 0$	$kd \to \infty$
$sinh(kd)$	kd	$e^{kd}/2$
$cosh(kd)$	1	$e^{kd}/2$
$tanh(kd)$	kd	1

First, let us recall the result for the wave profile (2.24). As already stated, this relationship means, that by this theory, the waves have a sinusoidal pattern. However experimental observations suggest, that the wave propagation is trochoidal.

Remark. Trochoid is the curve traced out by a point on a circle as the circle is rolled along a line.

The trochoidal wave approaches the sinusoidal shape for small amplitudes, however as can be seen in (fig. 2.6), even then the trochoid is distinguished by narrower peaks. The steepness of a wave becomes more pronounced as the amplitude increases.

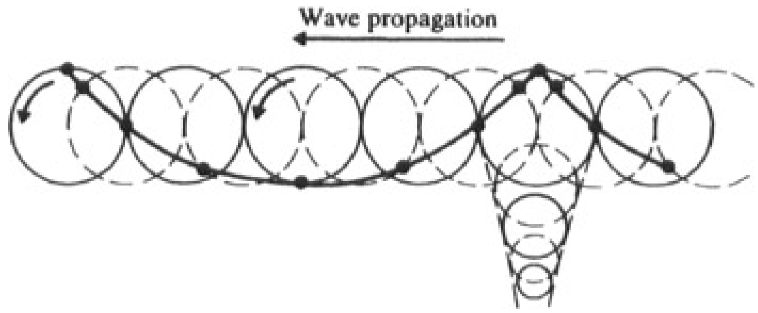

Figure 2.6: *Trochoidal progression of a wave.* Image downloaded from https://www.globalspec.com/reference/79955/203279/chapter-eleven-radar-remote-sensing

Second, we will discuss the expression for the phase speed as stated in (2.28). If we consider the case of a deep water (see 2.4.2), then

$$tanh(kd) \approx 1 \qquad \Longrightarrow \qquad c^2 = \frac{g}{k}.$$

On the other hand, if we now take the case of a shallow water, the situation is

$$tanh(kd) \approx kd \qquad \Longrightarrow \qquad c^2 = gd.$$

This means, that the phase velocity of the waves doesn't depend on the depth of the ocean in deep waters and in case of a shallow water, the velocity isn't influenced by the wavelength (respectively by the wave number).

However it has to stressed, that theses two cases are somewhat limit cases and the values of *tanh* are only approximations, so the velocity of both the shallow water waves and the deep water waves depend on both factors, the depth and the wavelength, although only one of them is dominant. We can observe from (2.28), that the phase speed varies with depth. For given values ω and k, the waves will propagate faster in deep waters than in shallow waters. The phase speed is also a function of k and from (2.27) can be seen, that waves with a longer wavelength will propagate faster than the ones with a shorter wavelength.

Lastly, we will make some observations about the motion of fluid particles based on (2.34).This equation represents an ellipse with the horizontal semi-axis A and the vertical semi-axis B. Thus in the linear wave theory, wave particles move in elliptical orbits. If we look at the definitons of A and B, we can observe, that in case of the deep water waves (i.e. $kd \to \infty$), they are identical, which means, the orbit is a circle. The orbits are circular throughout the water column, but decrease in diameter the deeper they are below the water surface.

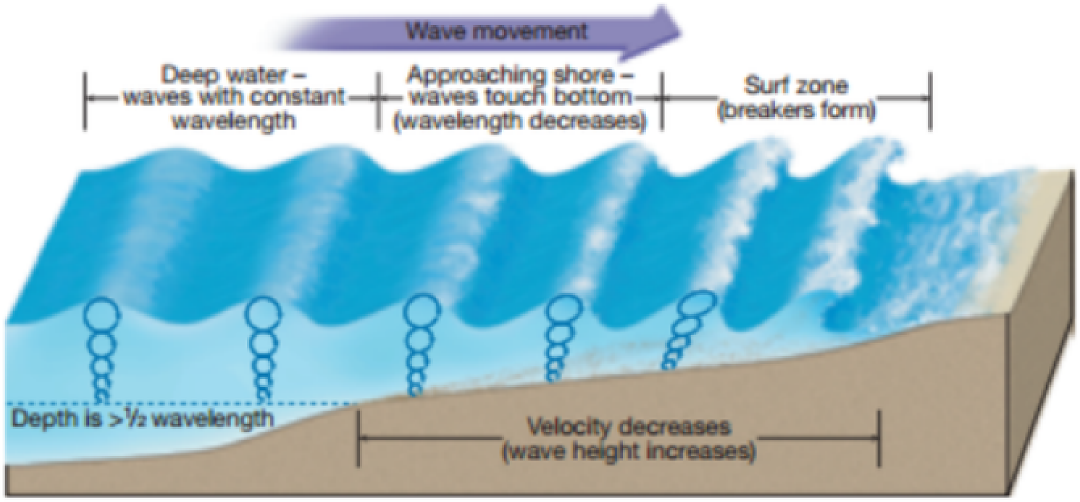

Figure 2.7: *Circular and elliptical orbits of water particles.* Image downloaded from https://wavestides.weebly.com/wave-motion.html

The figure 2.7 quite nicely shows, how the depth of sea influences the shape of the water particles. Their motion in a deep water is close to circular, however as the wave approaches the shore, the influence of a sea bed arises and starts to deform the orbits into ellipses.

This is the reason, why we distinguished between a shallow and a deep waters (2.4.2) based on the depth and the wavelength. The waves, where $d/L > 1/2$ don't "feel" the bottom, so the water particles move orderly in a circular pattern around a fixed position. The radius of their circular orbits is equal to the amplitude of the wave.

When the depth decreases below a half of the wavelength, the shape of the wave is deformed by the sea bed. The circular orbits of the water particles are changed into ellipses, which align to the shape of the bed. The ellipses in the water column become flatter near the sea bed. At the bottom, the particles follow a reversing horizontal path (due to the assumed irrotational motion). Also other characteristics start to change. As the bed rises, the amplitude of the wave increases, the wave slows down, but the period stays the same.

2.4.4. Generation of the Wind Waves

The wind waves arise by the wind acting on a water surface. The wind transfers energy to the waves as long as its speed is greater than the propagation speed of the waves. Beside a velocity, the creation of the wind waves is influenced by the duration of the wind and the *fetch* (i.e. a distance along which the wind maintains the same direction of blowing). The longer the fetch is, the bigger the waves are.

First, only small capillary waves (see 2.4.2) are generated on the surface, however as they overcome the surface tension, they transform into the gravitational waves. The capillary waves are caused due to small fluctuations in the wind speed, which result in variations in air pressure on the surface. Faster wind speeds produce a lower pressure and vice-versa (can be observed from the Bernoulli's equation). As the wind blows over the crests of the waves, the velocity profile near the surface increases, which results in a lower pressure. The opposite is true, when the wind passes the troughs.

According to some literature, the critical wind speed, which is needed for the observation of the gravity waves, is around 6.5 m/s.

2.4.5. Behaviour of the Waves

In this last part of this chapter, we will briefly look at how the waves interact with each other and with solid obstacles like a shore, since these interactions should be at least considered, when trying to describe the wave motion.

Wave Breaking

A wave can break at any water depth, provided it has a sufficient height. We can observe wave breaking especially near a shore, because as the wave crosses from a deep water into a shallow water, the sea bed starts to deform the wave. As already mentioned in (2.4.3), due to the energy loss caused by friction, the wave slows down, the amplitude increases and the wavelength is shortened. At certain wave height, the surface tension is no longer capable to hold the wave together and the wave breaks. Miche (1944) proposed a simple equation to determine, when the wave breaks

$$\left(\frac{H}{L}\right)_{max} = \frac{1}{7}\,tanh\left(\frac{2\pi d}{L}\right),$$

where H is the wave height, L is the wavelength and d is the depth. This rule is a good indication of wave breaking in deep waters, but not so accurate in shallow waters, because it doesn't consider the slope of a sea bed.

Usually the equation is simplified for deep waters into the form

$$\left(\frac{H}{L}\right)_{max} = \frac{1}{7}.$$

The reader can recall, that the expression on the left hand side is the steepness (2.4.1) and it is often stated in literature, that if the steepness of the wave exceeds this ratio, the wave will break.

For the shallow water waves, the original equation is approximately reduced to

$$\left(\frac{H}{L}\right)_{max} = \frac{1}{7}\,\frac{2\pi d}{L}$$

or also

$$\left(\frac{H}{d}\right)_{max} = 0.9.$$

The last expression tell us, that in case of shallow water waves, the height is restricted by the depth. This means, that the highest wave (generated in deep waters), that can approach the shore, is primarily given by the depth of the coast. This fact is considered, when building structures near shores.

From the modelling point of view, wave breaking creates a problem, because as the wave breaks, the motion is turbulent, which is difficult to describe. There are several types of wave breaking, but we will omit the list in this thesis, since it is not of a great importance for its purposes.

Refraction

The refraction means, that the wave bends towards the coast. This is due to the fact, that the waves only seldom approach the shore directly, but usually approach the coastline under some angle. However as part of the wave comes to the shallow water, this part of the wave slows down. This phenomenon appears to an observer standing on the shore as if the wave suddenly bended towards him.

More generally, the refraction occurs, when the waves pass from one medium to another (in this case the environment of a shallow and a deep water). The effect of refraction is important especially for tsunamis due to their very long wavelength. Thus they are refracted towards the land even afar from it.

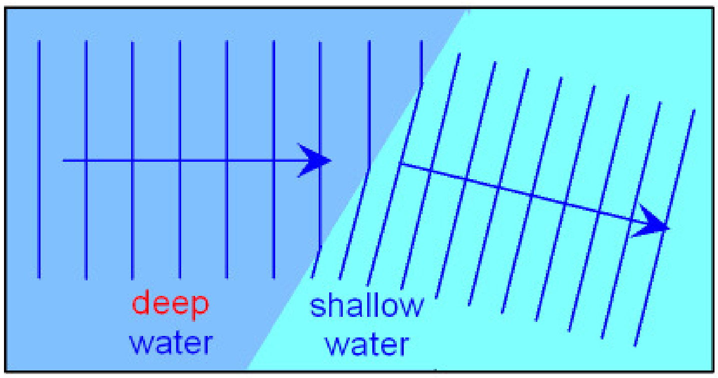

Figure 2.8: *The wave refraction.* Image downloaded from http://www.gcsescience.com/pwav42.htm

Diffraction

The wave diffraction can be described as a change of the direction of the waves when moving around objects or passing through holes. This can be for instance observed, as the waves pass between the barriers into a harbour.

The water waves have the ability to pass around the corners and obstacles, however as they do, the water behind these objects becomes disturbed and this causes the diffraction. This effect is influenced by the wavelength of the waves. Waves with longer wavelengths diffract more than the ones with short wavelengths. If the wavelength of a wave is smaller than the object the wave passes, the diffraction will not even occur. For example in harbour, the waves can diffract around smaller boats, however the same wave with the same wavelength will not diffract around greater ships there. The magnitude of the diffraction is also dependant on the size of a hole, where the water comes through. Smaller gaps produce greater diffraction. The diffraction can be observed in fig.2.9

Reflection

The reflection simply involves a change of directions as the wave bounces off an obstacle. The situation is given by the *law of reflection*. This law states, that

- The incident ray, the reflected ray (the rays are drawn perpendicular to the wave-fronts) and the normal to the reflection surface at the point of incidence lie in the same plane

Figure 2.9: *The wave diffraction.* Image downloaded from
http://physics.highpoint.edu/ jregester/potl/Waves/DiffractionInterference/Diffraction.html

- The angles of the incident and the reflected ray to the same normal are equal
- These two angles lie on the opposite sides of the normal

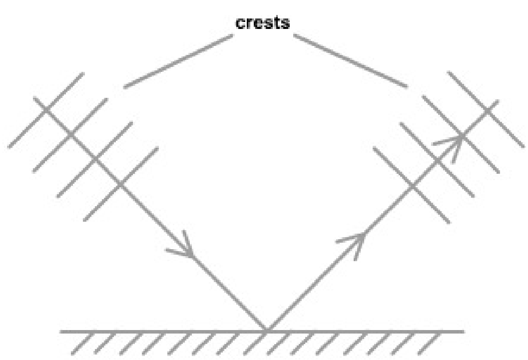

Figure 2.10: *The wave reflection.* Image downloaded from
http://www.bbc.co.uk/bitesize/higher/physics/radiation/waves/revision/1/

Wave Interference

Interference is a phenomenon, when two waves superimpose to form a resultant wave of a greater or a lower amplitude. The interference can even result in the waves cancelling each out or in forming the *standing waves*. In such case the wave appears to an observer as not moving (thus the term standing), but only vibrating up and down.

Whether the interference of the waves is constructive (the amplitude is magnified) or destructive (the amplitude is lowered), depends on whether the two waves have the same or the opposite phase.

However, the wave interference requires for the two waves to have the same frequency and the same phase throughout, which is viable in laboratory experiments or smaller regions, however when considering such macroscopic area as an ocean, meeting these requirements is not likely and thus the wave interference is of no great interest to us.

3. Considered Mathematical Models of Ocean Waves

The purpose of this chapter is to summarize several approaches, which we considered as possible ways to describe ocean waves in a coastal region.

In the first section, we describe the Boussinesq equations. The second section is dedicated to the Mild slope equation. The third section introduces the Shallow water equations. In the last part of this chapter, we discuss the chosen model for further study.

3.1. Boussinesq Equations

Boussinesq-type equations are derived from the three-dimensional Euler equations by the depth integration using a polynomial approximation for the vertical component of the velocity. The Boussinesq equations assume a weak non-linearity. The advantage of using the Boussinesq equations instead of the original Euler equations is, that in the former case we now have only two-dimensional problem (or more precisely, the two-dimensional approximation).

Several softwares were developed for a simulation of flows and waves based on the Boussinesq equations. Among some of such tools belong MIKE 21 (2001), FUNWAVE (1998) or BOUSS-2D (2007).

First considered equations to model the coastal waves were the *standard Boussinesq equations*, presented for the first time by Peregrine (1967) [14].

$$\eta_t + \nabla \cdot [(\eta + d)\boldsymbol{u}] = 0$$

$$\boldsymbol{u}_t + \frac{1}{2}\nabla|\boldsymbol{u}|^2 + g\nabla\eta + \frac{d^2}{6}\nabla(\nabla \cdot \boldsymbol{u}_t) - \frac{d}{2}\nabla(\nabla \cdot (d\boldsymbol{u}_t)) = 0,$$

where $\boldsymbol{u}$ is the depth averaged velocity, η is the function of free surface, d is the depth measured from the mean sea level and g is the gravitational acceleration.One of the major limitations of these equations is their restriction into a shallow water depths, where the vertical velocity approximation remains valid. They are not applicable in a very shallow water depths as well, because there the weak non-linearity assumption is no longer acceptable.

To extend the range of application of the standard Boussinesq equations, the *extended* or *modified Boussinesq equations* were presented by Nwongu (1993) [12].

$$\eta_t + \nabla \cdot [(\eta + d)\boldsymbol{u}_\alpha] + \nabla \cdot \left[\left(\frac{z_\alpha^2}{2} - \frac{d^2}{6}\right)d\nabla(\nabla \cdot \boldsymbol{u}_\alpha) + \left(z_{\alpha+}\frac{d}{2}\right)d\nabla(\nabla \cdot d\boldsymbol{u}_{\boldsymbol{\alpha}})\right] = 0$$

$$\boldsymbol{u}_{\boldsymbol{\alpha t}} + \frac{1}{2}\nabla|\boldsymbol{u}_{\boldsymbol{\alpha}}|^2 + g\nabla\eta + z_\alpha\left[\frac{1}{2}z_\alpha\nabla(\nabla \cdot \boldsymbol{u}_{\boldsymbol{\alpha t}}) + \nabla(\nabla \cdot (d\boldsymbol{u}_{\boldsymbol{\alpha t}}))\right] = 0,$$

where $z_\alpha = -0.531d$ and $\boldsymbol{u}_{\boldsymbol{\alpha}}$ is the horizontal velocity vector at the depth $z = z_\alpha$. The modified Boussinesq equations extended the application from the shallow water depths to an intermediate depths, where the ratio between the depth and the wavelength was close to 0.5. However these equations still suffer from the weak non-linearity restriction, which produces inaccurate results, as the wave approaches the shore and the wave height increases.

To even further extend the application, the weak non-linearity assumption can be removed. In such case the *fully non-linear Boussinesq equations* are obtained. Since these equations are even more complicated than the previous ones, we kindly refer the reader for more detailed study to [19], where the non-linear Boussinesq equations were presented by Wei (1995).

The original Boussinesq equations were derived under the assumptions of the irrotational motion of an incompressible, homogeneous, inviscid fluid. They can be used for modelling the effects of shoaling, refraction, diffraction and reflection of the shallow water waves.

3.2. Mild Slope Equation

The mild-slope approximation was introduced as a way of approximating the refraction and diffraction of linearized surface waves. Similarly to Boussinesq equations (3.1), the vertical component of the wave motion is averaged and thus the equations are again desirable due to their two-dimensional nature. As the name suggests, the equation is valid for mild-slope sea beds. More precisely, Booij (1983) [3] concluded, that the equation is valid up to the bottom slope 1:3.

Nowadays, for instance the code ARTEMIS inside the modelling software TELEMAC is based on solving the Mild-slope equation.

The *Mild-slope equation* proposed by Berkhoff (1976) [2] takes form

$$\frac{\partial}{\partial x}\left(p\frac{\partial \xi}{\partial x}\right) + \frac{\partial}{\partial y}\left(p\frac{\partial \xi}{\partial y}\right) + k^2 p\xi = 0,$$

where $k(x, y)$ is the local wave number and $\xi(x, y)$ is the complex-valued free surface displacement function.

The wave number k is determined from

$$\omega^2 = gk\, tanh(kd)$$

as the unique positive real root for given value of the angular velocity ω. The depth is denoted by $d(x, y)$, measured from the mean sea level.

The function $p(x, y)$ is defined as

$$p(x, y) = c(x, y)c_g(x, y).$$

The function $c(x, y)$ is the phase speed, which we already encountered in (2.4.3). It is given by

$$c = \frac{\omega}{k} = \sqrt{\frac{g}{k} tanh(kd)}$$

and $c_g(x, y)$ is called the *group velocity*, which is defined as

$$c_g = \frac{d\omega}{dk} = \frac{1}{2}c\left(1 + \frac{2kd}{sinh(2kd)}\right).$$

Since $\xi(x,y)$ is a complex-valued function, we can get the real-valued and time dependant free surface displacement $\eta(x,y,t)$ through the expression

$$\eta(x,y,t) = Re\{\xi(x,y)e^{-i\omega t}\}.$$

The Mild-slope equation was derived from the Navier-Stokes equation under the assumptions of a low value of bottom slope and a low value of wave steepness. Also the flow was assumed to be irrotational, the fluid incompressible and inviscid and the pressure on the free surface was supposed to be zero.

This equation is elliptic, however, if it can be assumed, that the waves propagate mainly in one direction, the parabolic approximations [9] can be made. This is a desirable solution, since the problem becomes one-dimensional. Also, the parabolic approximation is very convenient for computational purposes.

3.3. Shallow Water Equations

The last considered set of equations are the well known *Shallow water equations.* They are the usual model for description of a flow in rivers, channels and coastal areas. Apart from their application in the shallow water regions, they are commonly used also to describe the behaviour of an ocean or for debris flow simulation. One of the main areas of their application is the study of tsunamis. As already mentioned in (2.4.2), the tsunamis are distinguished by very long wavelengths. Since the depth of water is defined relatively with respect to the wavelengths, even such large waves as tsunamis can be considered "shallow" far from a shore. In case of an unidirectional flow, the Shallow water equations are also called the *Saint-Venant equations.*

Even though these equations are sometimes considered as too simplistic, they are used for modelling up to this day. We can see their application for example in the system FullSWOF.

The two-dimensional Shallow water equations are in the form

$$\begin{aligned} \frac{\partial h}{\partial t} + \frac{\partial (hu)}{\partial x} + \frac{\partial (hv)}{\partial y} &= 0 \\ \frac{\partial (hu)}{\partial t} + \frac{\partial (hu^2 + gh^2/2)}{\partial x} + \frac{\partial (huv)}{\partial y} &= 0 \\ \frac{\partial (hv)}{\partial t} + \frac{\partial (huv)}{\partial x} + \frac{\partial (hv^2 + gh^2/2)}{\partial y} &= 0. \end{aligned} \tag{3.1}$$

The first equation represents the conservation of mass and the second together with the third the conservation of momentum with respect to x and y. The right hand sides of the equations represent the source terms (a wind, an influence of a bed slope, a rain, a surface tension,...). In our case, we let the equations for the main part of the thesis to be homogeneous (i.e. no source terms are considered) and we will discuss most of the source terms later (in the chapter 7).

In the equations, u and v represent the horizontal (depth averaged) components of the velocity with respect to the x and y directions. The total height of a water column at certain point of the domain is denoted by $h = \eta - b$, where b is profile of the sea bed and η is the function of a free surface, measured from the plane $z = 0$ (fig. 3.1). The gravitational acceleration assumes the standard notation g.

There are several ways to derive the two-dimensional Shallow water equations and one of them is from the Navier-Stokes equation by depth integration under the assumption, that the horizontal length scale is much greater than the vertical one. That allows for the dimension reduction. The wavelength of the waves is assumed to be much larger than the depth of ocean. Other assumptions are incompressibility, constant temperature of the water, Newtonian fluid, the flow is inviscid, irrotational and not turbulent.

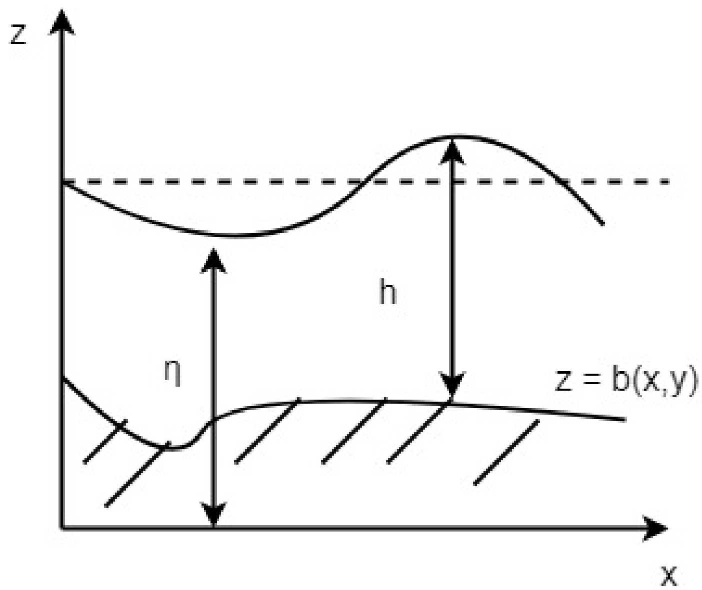

Figure 3.1: *Notation of Shallow water equations.*

3.4. Chosen Approach

We have chosen to base our model on the Shallow water equations, since they are not as complex as the Boussinesq and Mild-Slope equations. For that reason, the remainder of the thesis will be focused on the study and numerical solution of the Shallow water equations. We will consider the equations to be homogeneous for the most part of the work and introduce the source terms only in later stages.

4. Derivation and Analysis of Shallow Water Equations

In the first section of this chapter we will derive the Shallow water equations. In the second section we state possible forms of the governing equations. The third section is dedicated to the study of eigenvalues of the system. In the fourth section we classify the equations with respect to the results of the previous section.

4.1. Derivation of the Shallow Water Equations

4.1.1. Conservation of Mass

First, let us derive the conservation of mass. We will use both the *Reynold's kinematic transport* and *Gauss's theorems*, so let's recall them here.

Suppose, we have a material volume $V(t)$, bounded by $S(t)$, the volume $V(t)$ moves with the velocity vector $\boldsymbol{u}$ and $F(\boldsymbol{x}, t)$ is a fluid property.

Then the kinematic transport theorem states

$$\frac{D}{Dt}\int\limits_{V(t)} F \,\mathrm{d}V = \int\limits_{V(t)} \frac{\partial F}{\partial t}\,\mathrm{d}V + \int\limits_{S(t)} F\boldsymbol{u}\cdot\boldsymbol{n}\,\mathrm{d}S, \tag{4.1}$$

where $\frac{D}{Dt}$ denotes the material derivative

$$\frac{D}{Dt} = \frac{\partial}{\partial t} + \boldsymbol{u}\cdot\nabla. \tag{4.2}$$

To meet the assumptions of the Gauss's (also called *divergence*) theorem, let $S(t)$ be a compact and piecewise smooth boundary and let $\boldsymbol{F}$ be a continuously differentiable vector field defined on $V(t)$. The theorem then states

$$\int\limits_{V(t)} (\nabla\cdot\boldsymbol{F})\,\mathrm{d}V = \oint\limits_{S(t)} (\boldsymbol{F}\cdot\boldsymbol{n})\,\mathrm{d}S, \tag{4.3}$$

where the integral on the right hand side is the surface integral over the boundary $S(t)$.

Using the divergence theorem (4.3), we can rewrite the transport theorem (4.1) in the form

$$\frac{D}{Dt}\int\limits_{V(t)} F\,\mathrm{d}V = \int\limits_{V(t)} \frac{\partial F}{\partial t} + \nabla\cdot(F\boldsymbol{u})\,\mathrm{d}V \tag{4.4}$$

Now suppose $A(t)$ is an area in the (x, y) plane, which contains the same particles as it moves around with the horizontal velocity $\boldsymbol{u}(x, y, t) = (u, v)$. Let us imagine a column of water perpendicular to the (x, y) plane and $A(t)$ is the orthogonal projection of this column into the (x, y) plane. The column is of height $h(x, y, t)$ at given point of the plane (x, y). Also, let us assume, the water is incompressible, thus the density ρ is constant (i.e.

it is independent of time and space - see 2.3.2). Then we can express the total mass in such column as

$$\int_{A(t)} \rho h \, \mathrm{d}A.$$

We require, that the water column mass remains conserved, which means, that the rate at which the mass changes is zero. It is the material derivative, which describes the rate of change of some quantity with time in the continuum mechanics. We can capture this requirement by

$$\frac{D}{Dt} \int_{A(t)} \rho h \, \mathrm{d}A = 0. \tag{4.5}$$

If we apply the transport theorem (4.4) to (4.5) (we can since the theorem is valid not only for three dimensions), we obtain

$$\frac{D}{Dt} \int_{A(t)} \rho h \, \mathrm{d}A = \int_{A(t)} \frac{\partial(\rho h)}{\partial t} + \nabla \cdot (\rho h \boldsymbol{u}) \, \mathrm{d}A = 0. \tag{4.6}$$

Since the area $A(t)$ was arbitrary and assuming continuity of the integrand in (4.6), the integrand must vanish identically. For that reason we can say, that

$$\frac{\partial(\rho h)}{\partial t} + \nabla \cdot (\rho h \boldsymbol{u}) = 0. \tag{4.7}$$

Since we assumed, that the water is incompressible, the density can be taken out of the derivatives and we can divide the equation by it. Then (4.7) takes the form

$$\frac{\partial h}{\partial t} + \nabla \cdot (h \boldsymbol{u}) = 0. \tag{4.8}$$

The equation is (4.8) is equivalent to

$$\frac{\partial h}{\partial t} + \frac{\partial(hu)}{\partial x} + \frac{\partial(hv)}{\partial y} = 0, \tag{4.9}$$

which is the form of the conservation of mass as we presented it in (3.3).

4.1.2. Conservation of Momentum

For the derivation of the equations representing the conservation of momentum, we will use the Navier-Stokes equation for incompressible flows. The equation of motion is in the form

$$\rho \frac{\partial \boldsymbol{u}}{\partial t} + \rho(\boldsymbol{u} \cdot \nabla)\boldsymbol{u} = -\nabla p + \mu \nabla^2 \boldsymbol{u} + \rho \boldsymbol{g}, \tag{4.10}$$

where ρ is the density (assumed constant), $\boldsymbol{u} = (u, v, w)$ is the velocity vector, p is the pressure, μ is the dynamic viscosity and g is the gravitational acceleration. The conservation of mass (also *mass continuity*) equation in case of a three-dimensional incompressible flows is

$$\nabla \boldsymbol{u} = \frac{\partial u}{\partial x} + \frac{\partial v}{\partial y} + \frac{\partial w}{\partial z} = 0. \tag{4.11}$$

We will assume an inviscid flow, therefore (4.10) will reduce to

$$\rho \frac{\partial \boldsymbol{u}}{\partial t} + \rho(\boldsymbol{u} \cdot \nabla)\boldsymbol{u} = -\nabla p + \rho \boldsymbol{g}.$$

Next we divide the equation by the density ρ. Thus we obtain

$$\frac{\partial \boldsymbol{u}}{\partial t} + (\boldsymbol{u} \cdot \nabla)\boldsymbol{u} = -\frac{1}{\rho}\nabla p + \boldsymbol{g}. \tag{4.12}$$

We can expand (4.12) into the Cartesian coordinates (x, y, z) and (u, v, w), where each line represents the x, y and z - component of the equation.

$$\begin{aligned}
\frac{\partial}{\partial t}u + u\frac{\partial}{\partial x}u + v\frac{\partial}{\partial y}u + w\frac{\partial}{\partial z}u &= -\frac{1}{\rho}\frac{\partial}{\partial x}p \\
\frac{\partial}{\partial t}v + u\frac{\partial}{\partial x}v + v\frac{\partial}{\partial y}v + w\frac{\partial}{\partial z}v &= -\frac{1}{\rho}\frac{\partial}{\partial y}p \\
\frac{\partial}{\partial t}w + u\frac{\partial}{\partial x}w + v\frac{\partial}{\partial y}w + w\frac{\partial}{\partial z}w &= -\frac{1}{\rho}\frac{\partial}{\partial z}p - g
\end{aligned} \tag{4.13}$$

The left hand sides of the equations are equivalent to the material derivatives (4.2) of the velocity components u, v and w. With that in mind, let us rewrite the equations (4.13) into

$$\begin{aligned}
\frac{\partial}{\partial t}u + u\frac{\partial}{\partial x}u + v\frac{\partial}{\partial y}u + w\frac{\partial}{\partial z}u &= -\frac{1}{\rho}\frac{\partial}{\partial x}p \\
\frac{\partial}{\partial t}v + u\frac{\partial}{\partial x}v + v\frac{\partial}{\partial y}v + w\frac{\partial}{\partial z}v &= -\frac{1}{\rho}\frac{\partial}{\partial y}p \\
\frac{D}{Dt}w &= -\frac{1}{\rho}\frac{\partial}{\partial z}p - g.
\end{aligned} \tag{4.14}$$

One of the main assumption made during the derivation of shallow water equations is, that the horizontal scale is much larger, that the vertical one. If d is the depth measured from the mean sea level and L is the wavelength, we mean

$$\frac{d}{L} \ll 1.$$

Due to this assumption, we also assume any vertical motion can be neglected, in particular

$$\frac{D}{Dt}w = 0. \tag{4.15}$$

If we use the assumption (4.15), we can rewrite (4.14) as

$$\begin{aligned}
\frac{\partial}{\partial t}u + u\frac{\partial}{\partial x}u + v\frac{\partial}{\partial y}u + w\frac{\partial}{\partial z}u &= -\frac{1}{\rho}\frac{\partial}{\partial x}p \\
\frac{\partial}{\partial t}v + u\frac{\partial}{\partial x}v + v\frac{\partial}{\partial y}v + w\frac{\partial}{\partial z}v &= -\frac{1}{\rho}\frac{\partial}{\partial y}p \\
0 &= -\frac{1}{\rho}\frac{\partial}{\partial z}p - g.
\end{aligned} \tag{4.16}$$

Now, let's have a closer look at the z-component equation

$$\begin{aligned}
0 &= -\frac{1}{\rho}\frac{\partial}{\partial z}p - g \\
\frac{\partial}{\partial z}p &= -\rho g.
\end{aligned} \tag{4.17}$$

Denoting by η (for clarity see the fig. 3.1) the free water surface and p_a the atmospheric pressure, let us integrate (4.17) and thus obtain the pressure profile.

$$p = g\int_z^\eta \rho \,\mathrm{d}z + p_a \tag{4.18}$$

Since we have assumed an incompressible flow, the equation (4.18) is simplified to

$$p = \rho g(\eta - z) + p_a. \tag{4.19}$$

As we can observe, under the assumption (4.15), the pressure is hydrostatic, as if the flow was in rest. Now we compute the other spatial derivatives of (4.19).

$$\begin{aligned}
\frac{\partial}{\partial x}p &= \rho g\frac{\partial}{\partial x}\eta \\
\frac{\partial}{\partial y}p &= \rho g\frac{\partial}{\partial y}\eta
\end{aligned} \tag{4.20}$$

If we substitute (4.20) into (4.16), we obtain

$$\begin{aligned}
\frac{\partial}{\partial t}u + u\frac{\partial}{\partial x}u + v\frac{\partial}{\partial y}u + w\frac{\partial}{\partial z}u &= -g\frac{\partial}{\partial x}\eta \\
\frac{\partial}{\partial t}v + u\frac{\partial}{\partial x}v + v\frac{\partial}{\partial y}v + w\frac{\partial}{\partial z}v &= -g\frac{\partial}{\partial y}\eta.
\end{aligned} \tag{4.21}$$

The horizontal velocity components $u(x, y, t)$ and $v(x, y, t)$ can be interpreted as vertical mean velocities and are independent of z direction. Therefore

$$\frac{\partial}{\partial z}u = \frac{\partial}{\partial z}v = 0. \tag{4.22}$$

We can use the simplification (4.22) in the equations (4.21), so they are reduced to

$$\begin{aligned}
\frac{\partial}{\partial t}u + u\frac{\partial}{\partial x}u + v\frac{\partial}{\partial y}u &= -g\frac{\partial}{\partial x}\eta \\
\frac{\partial}{\partial t}v + u\frac{\partial}{\partial x}v + v\frac{\partial}{\partial y}v &= -g\frac{\partial}{\partial y}\eta.
\end{aligned} \tag{4.23}$$

The equations (4.23) are the non-conservative form of the momentum conservation equations. Their equivalent conservative form is

$$\begin{aligned}
\frac{\partial(hu)}{\partial t} + \frac{\partial(hu^2 + gh^2/2)}{\partial x} + \frac{\partial(huv)}{\partial y} &= -gh\frac{\partial}{\partial x}d \\
\frac{\partial(hv)}{\partial t} + \frac{\partial(huv)}{\partial x} + \frac{\partial(hv^2 + gh^2/2)}{\partial y} &= -gh\frac{\partial}{\partial y}d.
\end{aligned} \tag{4.24}$$

These equations are equivalent to the ones presented in (3.1) except for the fact, that now we have on the right hand side additional terms. These source terms represent the effect of bottom topography, namely the slope of bottom. If we neglect this influence, we will get the equations in to us already familiar form

$$\begin{aligned}
\frac{\partial(hu)}{\partial t} + \frac{\partial(hu^2 + gh^2/2)}{\partial x} + \frac{\partial(huv)}{\partial y} &= 0 \\
\frac{\partial(hv)}{\partial t} + \frac{\partial(huv)}{\partial x} + \frac{\partial(hv^2 + gh^2/2)}{\partial y} &= 0.
\end{aligned} \tag{4.25}$$

4.2. Governing Equations

The set of equations (4.9) and (4.25)

$$\begin{aligned}
\frac{\partial h}{\partial t} + \frac{\partial(hu)}{\partial x} + \frac{\partial(hv)}{\partial y} &= 0 \\
\frac{\partial(hu)}{\partial t} + \frac{\partial(hu^2 + gh^2/2)}{\partial x} + \frac{\partial(huv)}{\partial y} &= 0 \\
\frac{\partial(hv)}{\partial t} + \frac{\partial(huv)}{\partial x} + \frac{\partial(hv^2 + gh^2/2)}{\partial y} &= 0
\end{aligned} \tag{4.26}$$

is known as the *differential conservation form* of Shallow water equations. The conservation forms of equation signifies, that the corresponding physical quantity is conserved. In our case the mass and momentum.

For further analysis, it will be useful to introduce also the equivalent vector form of these equations.

$$\frac{\partial \boldsymbol{q}}{\partial t} + \frac{\partial \boldsymbol{F}}{\partial x} + \frac{\partial \boldsymbol{G}}{\partial y} = 0,$$

where

$$\boldsymbol{q} = \begin{bmatrix} h \\ hu \\ hv \end{bmatrix}, \quad \boldsymbol{F} = \begin{bmatrix} hu \\ hu^2 + gh^2/2 \\ huv \end{bmatrix}, \quad \boldsymbol{G} = \begin{bmatrix} hv \\ huv \\ hv^2 + gh^2/2 \end{bmatrix}. \tag{4.27}$$

In the vector form, the unknown $\boldsymbol{q}$ is the vector of conserved variables and $\boldsymbol{F}$ and $\boldsymbol{G}$ are the x and y components of the flux vector respectively.

Alternatively, the homogeneous Shallow water equations can be also written in the non-conserved variables (h, u, t) in the vector form as

$$\begin{aligned} &\frac{\partial}{\partial t} h + \boldsymbol{u} \cdot \nabla h + h \nabla \cdot \boldsymbol{u} = 0 \\ &\frac{\partial}{\partial t} \boldsymbol{u} + (\boldsymbol{u} \cdot \nabla) \boldsymbol{u} + g \nabla h = 0. \end{aligned}$$

4.3. Eigenvalues of the System

The motivation for studying the eigenvalues of the system of the homogeneous Shallow water equations is to prove, whether the system is hyperbolic or not. Since the system (4.27) is of the first order, we cannot assume the system to be neither elliptic nor parabolic, because such classification is for the second order linear PDE (see 2.1.3). The hyperbolicity of the system, if we can prove it, will be important for us later, when determining, which numerical method to use for the numerical algorithm.

Let us recall the equation system in the vector form

$$\frac{\partial \boldsymbol{q}}{\partial t} + \frac{\partial \boldsymbol{F}}{\partial x} + \frac{\partial \boldsymbol{G}}{\partial y} = 0,$$

where

$$\boldsymbol{q} = \begin{bmatrix} q_1 \\ q_2 \\ q_3 \end{bmatrix} = \begin{bmatrix} h \\ hu \\ hv \end{bmatrix}, \quad \boldsymbol{F} = \begin{bmatrix} hu \\ hu^2 + gh^2/2 \\ huv \end{bmatrix}, \quad \boldsymbol{G} = \begin{bmatrix} hv \\ huv \\ hv^2 + gh^2/2 \end{bmatrix}. \tag{4.28}$$

If we express $\boldsymbol{F}$ and $\boldsymbol{G}$ in terms of variables q_1, q_2 and q_3, we obtain

$$\boldsymbol{F} = \begin{bmatrix} q_2 \\ \dfrac{q_2^2}{q_1} + g\dfrac{q_1^2}{2} \\ \dfrac{q_2 q_3}{q_1} \end{bmatrix}, \quad \boldsymbol{G} = \begin{bmatrix} q_3 \\ \dfrac{q_2 q_3}{q_1} \\ \dfrac{q_3^2}{q_1} + g\dfrac{q_1^2}{2} \end{bmatrix}.$$

To compute the eigenvalues of Shallow water equations, we need to compute the Jacobian matrix of the vectors $\boldsymbol{F}(\boldsymbol{q}) = (f_1, f_2, f_3)$ and $\boldsymbol{G}(\boldsymbol{q}) = (g_1, g_2, g_3)$. By definition, the Jacobian matrix $\boldsymbol{F}'(\boldsymbol{q})$ of the vector $\boldsymbol{F}(\boldsymbol{q})$ is

$$\boldsymbol{F}'(\boldsymbol{q}) = \left[\frac{\partial f_i}{\partial q_j}\right] \quad for \quad i, j = 1, 2, 3.$$

Thus the Jacobian matrix looks like

$$\boldsymbol{F'}(\boldsymbol{q}) = \begin{bmatrix} \frac{\partial f_1}{\partial q_1} & \frac{\partial f_1}{\partial q_2} & \frac{\partial f_1}{\partial q_3} \\ \frac{\partial f_2}{\partial q_1} & \frac{\partial f_2}{\partial q_2} & \frac{\partial f_2}{\partial q_3} \\ \frac{\partial f_3}{\partial q_1} & \frac{\partial f_3}{\partial q_2} & \frac{\partial f_3}{\partial q_3} \end{bmatrix}$$

and analogically for $\boldsymbol{G}'(\boldsymbol{q})$. We can then write down the system (4.28) in the quasi-linear conservative form

$$\frac{\partial \boldsymbol{q}}{\partial t} + \boldsymbol{F'}(\boldsymbol{q})\frac{\partial \boldsymbol{q}}{\partial x} + \boldsymbol{G'}(\boldsymbol{q})\frac{\partial \boldsymbol{q}}{\partial y} = 0. \tag{4.29}$$

The computation of Jacobian matrices yields

$$\boldsymbol{F'}(\boldsymbol{q}) = \begin{bmatrix} 0 & 1 & 0 \\ gq_1 - \frac{q_2^2}{q_1^2} & \frac{2q_2}{q_1} & 0 \\ -\frac{q_2 q_3}{q_1^2} & \frac{q_3}{q_1} & \frac{q_2}{q_1} \end{bmatrix}$$

and

$$\boldsymbol{G'}(\boldsymbol{q}) = \begin{bmatrix} 0 & 0 & 1 \\ -\frac{q_2 q_3}{q_1^2} & \frac{q_3}{q_1} & \frac{q_2}{q_1} \\ gq_1 - \frac{q_3^2}{q_1^2} & 0 & \frac{2q_3}{q_1} \end{bmatrix}.$$

Since the system (4.29) is two-dimensional, the solutions (waves) will move in some direction given by the unit normal vector $\boldsymbol{n} = (n_x, n_y)$. The eigenvalues (according to [11]) can be computed by solving

$$|n_x\boldsymbol{F'}(\boldsymbol{q}) + n_y\boldsymbol{G'}(\boldsymbol{q}) - \lambda_i \boldsymbol{I}| = 0 \quad for \quad i = 1, 2, 3.$$

The detailed computation would be quite tedious, so we omit it here. However using the system *Wolfram Alpha*, we obtained the result

$$\begin{aligned} \lambda_1 &= -\frac{\sqrt{gq_1^5(n_x^2+n_y^2)} + n_x q_1 q_2 + n_y q_1 q_3}{q_1^2} \\ \lambda_2 &= \frac{n_x q_2 + n_y q_3}{q_1} \\ \lambda_3 &= \frac{\sqrt{gq_1^5(n_x^2+n_y^2)} + n_x q_1 q_2 + n_y q_1 q_3}{q_1^2}, \end{aligned}$$

which is equivalent (by keeping in mind $n_x^2 + n_y^2 = 1$) to the form

$$\begin{aligned}\lambda_1 &= n_x \frac{q_2}{q_1} + n_y \frac{q_3}{q_1} - \sqrt{g q_1} \\ \lambda_2 &= n_x \frac{q_2}{q_1} + n_y \frac{q_3}{q_1} \\ \lambda_3 &= n_x \frac{q_2}{q_1} + n_y \frac{q_3}{q_1} + \sqrt{g q_1}.\end{aligned} \tag{4.30}$$

We can also revert the eigenvalues to the non-conservative variables h, u, v and get

$$\begin{aligned}\lambda_1 &= \boldsymbol{n} \cdot \boldsymbol{u} - c \\ \lambda_2 &= \boldsymbol{n} \cdot \boldsymbol{u} \\ \lambda_3 &= \boldsymbol{n} \cdot \boldsymbol{u} + c,\end{aligned} \tag{4.31}$$

where $c = \sqrt{gh}$ is the phase speed (we can recall the formula (2.28), as it reduced for the shallow waters).

Remark. Actually, we derived from (2.28), that for the shallow water the phase speed is reduced to $c = \sqrt{gd}$ and not $c = \sqrt{gh}$. The difference arises from the fact, that in the linear wave theory, we assumed the height of the waves to be very small (going to 0) and thus $d \approx h$.

4.4. Hyperbolicity of Shallow Water Equations

From the computed eigenvalues (4.31)

$$\begin{aligned}\lambda_1 &= \boldsymbol{n} \cdot \boldsymbol{u} - \sqrt{gh} \\ \lambda_2 &= \boldsymbol{n} \cdot \boldsymbol{u} \\ \lambda_3 &= \boldsymbol{n} \cdot \boldsymbol{u} + \sqrt{gh},\end{aligned}$$

we can observe, that all the eigenvalues are real and distinct for $h > 0$. Thus the system (4.29) of Shallow water equations is *hyperbolic* (see 2.1.3). As we have mentioned in the beginning of the section (4.3), we will consider this fact, when choosing a numerical method for the numerical solution.

5. Numerical Solution of Shallow Water Equations

This chapter is dedicated to the formulation of Finite volume method and a proposal of numerical algorithm, which we will use to approximately solve the two-dimensional Shallow water equations.

The first section of this chapter discusses the chosen numerical method. The second section describes the Finite volume method in one-dimensional hyperbolic systems. The following third section does the same for two dimensions. The fourth section proposes a possible numerical scheme for the solution of the Shallow water equations. The last section includes a source term into the scheme.

5.1. Numerical Method Used in the Thesis

We will discuss here the choice of a numerical method with respect to the considered possibilities (2.2.2).

The approach of MOC is for us infeasible, since we will not find the characteristics in case of the two-dimensional Shallow water equations. Aside that, all three remaining approaches are valid to implement. Since we will due to the choice of a rectangular domain implement a structured rectangular mesh, perhaps FDM would be the easiest choice. However, we chose the node-centered Finite volume method, since we advise as a possible extension of the work the use of triangular meshes (more suitable for irregular or complex domains) and for that FVM is more convenient.

Also FVM is often used for hyperbolic equations, as is the case of Shallow water equations (see 4.4), because the hyperbolic equations are subjected to discontinuities in the solution (i.e. the dependant variables are discontinuous). These discontinuities are called *shock waves* and may arise even if the boundary and initial conditions are smooth. The Finite volume method is a suitable approach to deal with this obstacle. The formulation of FDM may fail near these discontinuities.

5.2. Finite Volume Method in the One-Dimensional Case

Let us consider a one-dimensional system of a conservation law written in the differential form as

$$\frac{\partial \boldsymbol{q}}{\partial t} + \frac{\partial \boldsymbol{F}(\boldsymbol{q})}{\partial x} = 0. \tag{5.1}$$

The differential form is valid only in the case, when the solution is smooth throughout. If there are discontinuities, we must use an integral form. An integral form for (5.1) is

$$\oint [\boldsymbol{q}\,\mathrm{d}x - \boldsymbol{F}(\boldsymbol{q})\,\mathrm{d}t] = 0,$$

where the line integration is performed along the boundary of the domain in an anticlockwise manner. By choosing a quadrilateral control volume V_i (see fig. 5.1) in the (x,t) plane

$$[x_{i-\frac{1}{2}}, x_{i+\frac{1}{2}}] \times [t_n, t_{n+1}],$$

we may write another expression of the integral form

$$\int_{x_{i-\frac{1}{2}}}^{x_{i+\frac{1}{2}}} \boldsymbol{q}(x,t_{n+1})\,\mathrm{d}x = \\ \int_{x_{i-\frac{1}{2}}}^{x_{i+\frac{1}{2}}} \boldsymbol{q}(x,t_n)\,\mathrm{d}x - \left[\int_{t_n}^{t_{n+1}} \boldsymbol{F}(\boldsymbol{q}(x_{i+\frac{1}{2}},t))\,\mathrm{d}t - \int_{t_n}^{t_{n+1}} \boldsymbol{F}(\boldsymbol{q}(x_{i-\frac{1}{2}},t))\,\mathrm{d}t\right]. \tag{5.2}$$

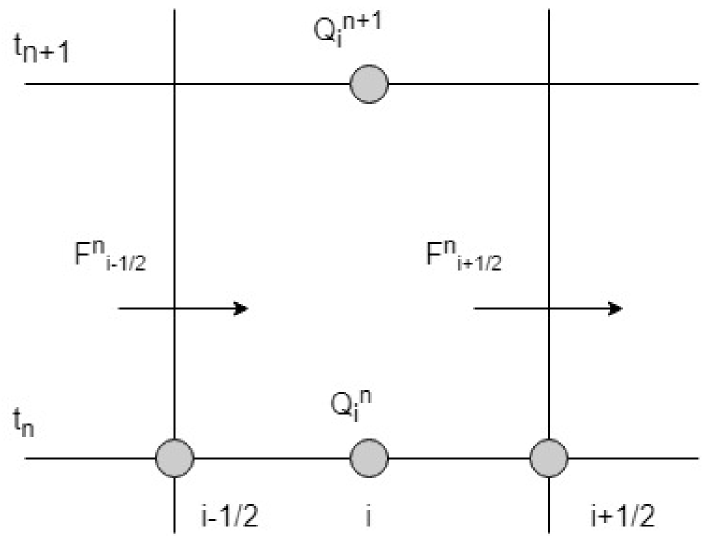

Figure 5.1: *Control volume V_i.*

Now we can define the mesh size Δx_i and the time step Δt as

$$\Delta x_i = x_{i+\frac{1}{2}} - x_{i-\frac{1}{2}} \quad \text{and} \quad \Delta t = t_{n+1} - t_n.$$

Let us divide the whole equation (5.2) by Δx_i and then multiply the part on the right hand side of the equation in square brackets by $\frac{\Delta t}{\Delta t}$. We obtain

$$\frac{1}{\Delta x_i}\int_{x_{i-\frac{1}{2}}}^{x_{i+\frac{1}{2}}} \boldsymbol{q}(x,t_{n+1})\,\mathrm{d}x = \\ \frac{1}{\Delta x_i}\int_{x_{i-\frac{1}{2}}}^{x_{i+\frac{1}{2}}} \boldsymbol{q}(x,t_n)\,\mathrm{d}x - \frac{\Delta t}{\Delta t \Delta x_i}\left[\int_{t_n}^{t_{n+1}} \boldsymbol{F}(\boldsymbol{q}(x_{i+\frac{1}{2}},t))\,\mathrm{d}t - \int_{t_n}^{t_{n+1}} \boldsymbol{F}(\boldsymbol{q}(x_{i-\frac{1}{2}},t))\,\mathrm{d}t\right]. \tag{5.3}$$

Now we define the cell integral averages of $\boldsymbol{q}(x,t)$ at times t_n and t_{n+1}. Since the length (volume) is Δx_i, we can define the cell averages $\boldsymbol{Q}_i^n$ and $\boldsymbol{Q}_i^{n+1}$ as

$$\boldsymbol{Q}_i^n = \frac{1}{\Delta x_i} \int_{x_{i-\frac{1}{2}}}^{x_{i+\frac{1}{2}}} \boldsymbol{q}(x, t_n) \mathrm{d}x$$
$$\boldsymbol{Q}_i^{n+1} = \frac{1}{\Delta x_i} \int_{x_{i-\frac{1}{2}}}^{x_{i+\frac{1}{2}}} \boldsymbol{q}(x, t_{n+1}) \mathrm{d}x. \tag{5.4}$$

The cell average $\boldsymbol{Q}_i^n$ is an approximated value of $\boldsymbol{q}(x, t_n)$ over the volume V_i.

Similarly, we will now define time integral averages of the flux $\boldsymbol{F(q)}$ at positions $x_{i-\frac{1}{2}}$ and $x_{i+\frac{1}{2}}$, specifically

$$\boldsymbol{F}_{\boldsymbol{i-\frac{1}{2}}} = \frac{1}{\Delta t} \int_{t_n}^{t_{n+1}} \boldsymbol{F}(\boldsymbol{q}(x_{i-\frac{1}{2}}, t)) \mathrm{d}t$$
$$\boldsymbol{F}_{\boldsymbol{i+\frac{1}{2}}} = \frac{1}{\Delta t} \int_{t_n}^{t_{n+1}} \boldsymbol{F}(\boldsymbol{q}(x_{i+\frac{1}{2}}, t)) \mathrm{d}t. \tag{5.5}$$

Using definitions (5.4) and (5.5), we can rewrite (5.3) as follows

$$\boldsymbol{Q}_i^{n+1} = \boldsymbol{Q}_i^n - \frac{\Delta t}{\Delta x_i} [\boldsymbol{F}_{\boldsymbol{i+\frac{1}{2}}} - \boldsymbol{F}_{\boldsymbol{i-\frac{1}{2}}}]. \tag{5.6}$$

The flux $\boldsymbol{F}_{\boldsymbol{i+\frac{1}{2}}}$ at $x_{i+\frac{1}{2}}$ between the cells V_i and V_{i+1} is called a *numerical flux* or an *intercellar flux.*

The numerical flux can be in general

$$\boldsymbol{F}_{\boldsymbol{i+\frac{1}{2}}} = \boldsymbol{F}_{\boldsymbol{i+\frac{1}{2}}}(\boldsymbol{Q}_{i-k_L}^n, ..., \boldsymbol{Q}_{i+k_R}^n),$$

where the non-negative integers k_L and k_R depend on the particular choice of the numerical flux.

In explicit methods, the arguments are evaluated at time t_n. In implicit methods, the arguments may also contain information from time t_{n+1}.

Since in hyperbolic systems the information propagates with finite speed, it's reasonable to assume, that we can compute $\boldsymbol{F}_{\boldsymbol{i+\frac{1}{2}}}$ based on the values of cell averages $\boldsymbol{Q}_{i+1}^n$ and $\boldsymbol{Q}_i^n$. Then we could write $\boldsymbol{F}_{\boldsymbol{i+\frac{1}{2}}}$ as

$$\boldsymbol{F}_{\boldsymbol{i+\frac{1}{2}}} = \mathbf{f}(\boldsymbol{Q}_i^n, \boldsymbol{Q}_{i+1}^n),$$

where $\mathbf{f}$ is some numerical flux.

The formula (5.6) would then become

$$\boldsymbol{Q}_i^{n+1} = \boldsymbol{Q}_i^n - \frac{\Delta t}{\Delta x_i} [\mathbf{f}(\boldsymbol{Q}_i^n, \boldsymbol{Q}_{i+1}^n) - \mathbf{f}(\boldsymbol{Q}_{i-1}^n, \boldsymbol{Q}_i^n)].$$

The specific numerical scheme would then depend on the choice of the function $\mathbf{f}$. That choice is important, since it is the numerical flux, which overcomes the discontinuities (see 2.2.3) arising in the FVM between cells.

Let us also here observe a property of this method (of conservative methods in general). It is called the *telescopic property*, which says, that the intercell flux $\boldsymbol{F}_{\boldsymbol{i+\frac{1}{2}}}$, used to update the cell average $\boldsymbol{Q}_i^n$, must be identical to the intercell flux $\boldsymbol{F}_{\boldsymbol{i-\frac{1}{2}}}$, used to update the cell average $\boldsymbol{Q}_{i+1}^n$. Thus on summation of $\boldsymbol{Q}_i^n$ and $\boldsymbol{Q}_{i+1}^n$ the flux at the boundary between the cells V_i and V_{i+1} cancels out. Let us assume a discretised domain with V_{Left} being the leftmost and V_{Right} the rightmost cells of such domain. Then multiply (5.6) by Δx_i and sum across the cells in this domain. We obtain

$$\sum_{i=Left}^{i=Right} \Delta x_i\, \boldsymbol{Q}_i^{n+1} = \sum_{i=Left}^{i=Right} \Delta x_i\, \boldsymbol{Q}_i^n - \Delta t\, [\boldsymbol{F}_{Right} - \boldsymbol{F}_{Left}].$$

Almost all intercellar fluxes cancelled out and we are left only with the rightmost $\boldsymbol{F}_{Right}$ and the leftmost $\boldsymbol{F}_{Left}$ intercellar fluxes. This means, that the total amount of conserved variable $\boldsymbol{q}$ changes only because of the fluxes through the end boundaries.

5.3. Finite Volume Method in the Two-Dimensional Case

Now we recall the differential conservative form of two-dimensional Shallow water equations

$$\frac{\partial \boldsymbol{q}}{\partial t} + \frac{\partial \boldsymbol{F}}{\partial x} + \frac{\partial \boldsymbol{G}}{\partial y} = 0,$$

where

$$\boldsymbol{q} = \begin{bmatrix} h \\ hu \\ hv \end{bmatrix}, \quad \boldsymbol{F} = \begin{bmatrix} hu \\ hu^2 + gh^2/2 \\ huv \end{bmatrix}, \quad \boldsymbol{G} = \begin{bmatrix} hv \\ huv \\ hv^2 + gh^2/2 \end{bmatrix}.$$

The corresponding integral form (using the divergence theorem after moving the fluxes on the other side of the equation) is

$$\frac{\mathrm{d}}{\mathrm{d}t} \iint_V \boldsymbol{q}\, \mathrm{d}V = -\int_\Omega \mathcal{H} \cdot \boldsymbol{n}\, \mathrm{d}\Omega, \tag{5.7}$$

where V is a control volume, Ω its boundary, $\mathcal{H} = (\boldsymbol{F}, \boldsymbol{G})$ is the vector of fluxes, $\boldsymbol{n} = (n_x, n_y)$ is the outward unit vector normal to the surface Ω.

The cell average $\boldsymbol{Q}$ over the volume V can be defined as

$$\boldsymbol{Q} = \frac{1}{|V|} \iint_V \boldsymbol{q}\, \mathrm{d}V, \tag{5.8}$$

where $|V|$ denotes the volume of V (the area of V, since we are in two spatial dimension).

Substituting (5.8) into (5.7) yields

$$|V| \frac{\mathrm{d}}{\mathrm{d}t} \boldsymbol{Q} = -\int_\Omega \mathcal{H} \cdot \boldsymbol{n}\, \mathrm{d}\Omega. \tag{5.9}$$

If we write the right hand side of (5.9) in term of sum and divide the equation by $|V|$, we obtain

$$\frac{\mathrm{d}}{\mathrm{d}t}\boldsymbol{Q} = -\frac{1}{|V|}\sum_{s=1}^{N}\mathcal{F}_s, \tag{5.10}$$

where

$$\mathcal{F}_s = \int_{A_s}^{A_{s+1}} [n_x\boldsymbol{F}(\boldsymbol{q}) + n_y\boldsymbol{G}(q)]\,\mathrm{d}\Omega. \tag{5.11}$$

The number of vertices of the particular shape of V is denoted by N and the subscript s signifies the cell's side, so the integration in (5.11) means an integration along the side of a cell.

By replacing the time derivative in (5.10) by a forward time approximation, we obtain fully discrete scheme

$$\boldsymbol{Q}_{i,j}^{n+1} = \boldsymbol{Q}_{i,j}^{n} - \frac{\Delta t}{|I_{i,j}|}\sum_{s=1}^{N}\mathcal{F}_s, \tag{5.12}$$

where $|I_{i,j}|$ is the area of the cell $I_{i,j}$. The notation I for cells is more common in two-dimensional case.

In case of a mesh grid made by perfect quadrilaterals (see fig. (5.2)) of area $\Delta x \times \Delta y$, the formula (5.12) is reduced to

$$\boldsymbol{Q}_{i,j}^{n+1} = \boldsymbol{Q}_{i,j}^{n} - \frac{\Delta t}{\Delta x}[\boldsymbol{F}_{i+\frac{1}{2},j} - \boldsymbol{F}_{i-\frac{1}{2},j}] - \frac{\Delta t}{\Delta y}[\boldsymbol{G}_{i,j+\frac{1}{2}} - \boldsymbol{G}_{i,j-\frac{1}{2}}]. \tag{5.13}$$

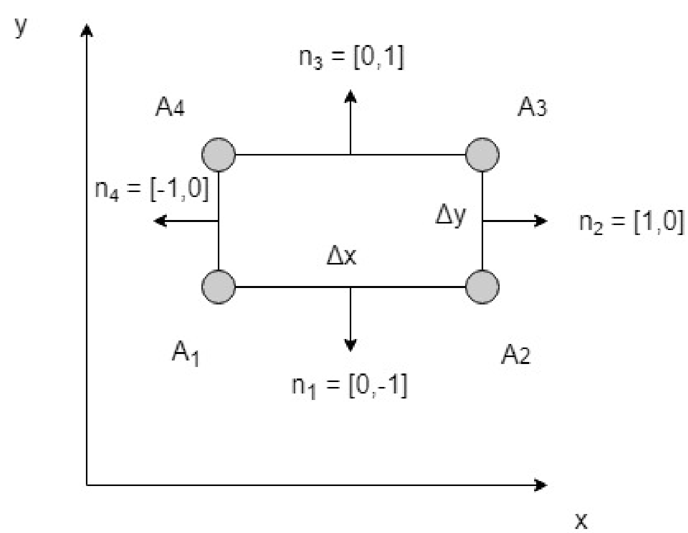

Figure 5.2: *Control volume $I_{i,j}$.*

Both results (5.6) and (5.13) can be found in numerous literature. We recommend for the study of FVM in fluid mechanics the books [16] and [5].

5.4. Numerical Scheme

Now we will focus more on the development of the numerical algorithm specifically for the Shallow water equations, which we have in form

$$\frac{\partial \boldsymbol{q}}{\partial t} + \frac{\partial \boldsymbol{F}}{\partial x} + \frac{\partial \boldsymbol{G}}{\partial y} = 0,$$

where

$$\boldsymbol{q} = \begin{bmatrix} h \\ hu \\ hv \end{bmatrix}, \quad \boldsymbol{F} = \begin{bmatrix} hu \\ hu^2 + gh^2/2 \\ huv \end{bmatrix}, \quad \boldsymbol{G} = \begin{bmatrix} hv \\ huv \\ hv^2 + gh^2/2 \end{bmatrix}.$$

We suppose the domain $\boldsymbol{D}$ is in (x, y) plane and the waves will propagate in time t. The variable $h(x, y, t)$ denotes the total height of the water column at given time and space and $(u(x, y, t), v(x, y, t))$ is the vertically averaged horizontal fluid velocity field. We will assume no source terms in the equation.

The initial value problem can be then written as

$$\frac{\partial \boldsymbol{q}}{\partial t} + \frac{\partial \boldsymbol{F}}{\partial x} + \frac{\partial \boldsymbol{G}}{\partial y} = 0$$
$$\boldsymbol{q}(\boldsymbol{x}, 0) = \boldsymbol{q}_0(\boldsymbol{x}), \quad \boldsymbol{x} = (x, y) \in \boldsymbol{D}, \quad t > 0.$$

The maximal directional wave velocities (in directions x and y), corresponding to the maximal eigenvalues of the Jacobian matrices

$$\frac{\partial \boldsymbol{F}}{\partial \boldsymbol{q}} \quad \text{and} \quad \frac{\partial \boldsymbol{G}}{\partial \boldsymbol{q}}$$

are (as can be seen from (4.31) for) given as

$$\lambda_x(\boldsymbol{q}) = |u| + \sqrt{gh} \tag{5.14}$$
$$\lambda_y(\boldsymbol{q}) = |v| + \sqrt{gh}. \tag{5.15}$$

We obtained these expressions for λ_x and λ_y, since for our structured mesh, we have $n_x = 1$ and $n_y = 0$ for the propagation in the x-direction and vice-versa for the y-direction.

Now, when we established some basics, let us first observe the incorporation of the chosen numerical flux into the obtained Finite volume formula in the one-dimensional case, so we understand the idea of computation and then we will return to the two-dimensional case, where the situation will not change that much.

5.4.1. One Dimension

One dimensional form of the Shallow water equations is

$$\frac{\partial \boldsymbol{q}}{\partial t} + \frac{\partial \boldsymbol{F}}{\partial x} = 0,$$

where

$$\boldsymbol{q} = \begin{bmatrix} h \\ hu \end{bmatrix}, \quad \boldsymbol{F} = \begin{bmatrix} hu \\ hu^2 + gh^2/2 \end{bmatrix}.$$

Thus the domain $\boldsymbol{D}$ is some interval I. Let us recall here the explicit formula

$$\boldsymbol{Q}_i^{n+1} = \boldsymbol{Q}_i^n - \frac{\Delta t}{\Delta x_i}[\boldsymbol{F}_{\boldsymbol{i+\frac{1}{2}}} - \boldsymbol{F}_{\boldsymbol{i-\frac{1}{2}}}] \tag{5.16}$$

as we have derived it (5.6).

The vector

$$\boldsymbol{Q_i^n} = \begin{bmatrix} h^n \\ (hu)_i^n \end{bmatrix}$$

denotes the cell average of the solution

$$\boldsymbol{q} = \begin{bmatrix} h \\ hu \end{bmatrix}.$$

There are numerous formulas for the numerical flux $\boldsymbol{F}_{\boldsymbol{i+\frac{1}{2}}}$ in (5.16), but in our paper, we will use the Rusanov numerical flux function

$$\boldsymbol{F}^n_{i+\frac{1}{2}}(\boldsymbol{Q}_i^n, \boldsymbol{Q}_{i+1}^n) \approx \boldsymbol{F}^{\mathrm{Rus}}(\boldsymbol{Q}_L, \boldsymbol{Q}_R) = \frac{(\boldsymbol{F}_L + \boldsymbol{F}_R)}{2} - \frac{\lambda_{max}}{2}(\boldsymbol{Q}_R - \boldsymbol{Q}_L), \tag{5.17}$$

thus

$$\boldsymbol{F}^n_{i+\frac{1}{2}}(\boldsymbol{Q}_i^n, \boldsymbol{Q}_{i+1}^n) \approx \frac{(\boldsymbol{F}_i^n + \boldsymbol{F}_{i+1}^n)}{2} - -\frac{\lambda_{max}}{2}(\boldsymbol{Q}_{i+1}^n - \boldsymbol{Q}_i^n).$$

The numerical flux $\boldsymbol{F}_{\boldsymbol{i-\frac{1}{2}}}$ si computed analogically from the values $\boldsymbol{Q}_{i-1}^n$ and $\boldsymbol{Q}_i^n$ using the Rusanov formula.

The local maximum wave speeds are denoted by λ_{max}, which is given as

$$\lambda_{max} = \max(\lambda_x(\boldsymbol{Q}_L), \lambda_x(\boldsymbol{Q}_R)) = \max(\lambda_x(\boldsymbol{Q}_i^n), \lambda_x(\boldsymbol{Q}_{i+1}^n)),$$

where λ_x is defined as in (5.14).

The mesh width Δx is

$$\Delta x = \frac{|I|}{N_x},$$

where N_x denotes the number of the mesh cells.

For the method to be stable, the time step has respect the CFL condition (2.5)

$$\Delta t = C_{\mathrm{CFL}}\frac{\Delta x}{\bar{\lambda}_x} \leq \frac{\Delta x}{\bar{\lambda}_x} = \frac{\Delta x}{\max\limits_i \lambda_x(\boldsymbol{Q}_i)},$$

where $0 < C_{\mathrm{CFL}} \leq 1$.

For implementing the boundary condition, we can extrapolate the values of variables to the ghost cells and set

$$\boldsymbol{Q}_0^n = \boldsymbol{Q}_1^n \quad \text{and} \quad \boldsymbol{Q}_{N_x+1}^n = \boldsymbol{Q}_{N_x}^n,$$

if both ends represent the free boundaries (see 2.1.2). In the case of the reflective boundaries, we set the ghost cells in the same way as for outflows, with the exception, that the velocity u must have an opposite sign. Meaning

$$\begin{aligned} \boldsymbol{Q}_0^n &= \boldsymbol{Q}_1^n \quad \text{and} \quad \boldsymbol{Q}_{N_x+1}^n = \boldsymbol{Q}_{N_x}^n, \\ u_0^n &= -u_1^n \quad \text{and} \quad u_{N_x+1}^n = -u_{N_x}^n. \end{aligned}$$

5.4.2. Two Dimensions

Now we extend the understanding of 1D formula to 2D. Similarly to the problem in one dimension, we recall the obtained result (5.13) from the previous section

$$\boldsymbol{Q}_{i,j}^{n+1} = \boldsymbol{Q}_{i,j}^n - \frac{\Delta t}{\Delta x}[\boldsymbol{F}_{i+\frac{1}{2},j} - \boldsymbol{F}_{i-\frac{1}{2},j}] - \frac{\Delta t}{\Delta y}[\boldsymbol{G}_{i,j+\frac{1}{2}} - \boldsymbol{G}_{i,j-\frac{1}{2}}]. \tag{5.18}$$

The domain $\boldsymbol{D}$ is now some rectangular area $\boldsymbol{D} = I_1 \times I_2$, where the interval I_1 is discretized into N_x cells and the interval I_2 into N_y.

Once again the vector

$$\boldsymbol{Q_{i,j}^n} = \begin{bmatrix} h_{i,j}^n \\ (hu)_{i,j}^n \\ (hv)_{i,j}^n \end{bmatrix}$$

approximates over a cell the exact solution

$$\boldsymbol{q} = \begin{bmatrix} h \\ hu \\ hv \end{bmatrix}.$$

Both numerical fluxes $\boldsymbol{F_{i+\frac{1}{2},j}}$ and $\boldsymbol{G_{i,j+\frac{1}{2}}}$ in (5.18) will be approximated by Rusanov flux, i.e.

$$\boldsymbol{F}_{i+\frac{1}{2},j}^n \approx \boldsymbol{F}^{\text{Rus}}(\boldsymbol{Q}_{i,j}^n, \boldsymbol{Q}_{i+1,j}^n) \quad \text{and} \quad \boldsymbol{G}_{i,j+\frac{1}{2}}^n \approx \boldsymbol{G}^{\text{Rus}}(\boldsymbol{Q}_{i,j}^n, \boldsymbol{Q}_{i,j+1}^n),$$

where the formulas for $\boldsymbol{F}^{\text{Rus}}$ and $\boldsymbol{G}^{\text{Rus}}$ are defined the same way as in the one-dimensional case (5.17). Except when computing the Rusanov approximation for the flux $\boldsymbol{G}$, we now have to use λ_y (given by 5.15) in the formula for λ_{max}. Again, the fluxes $\boldsymbol{F_{i-\frac{1}{2},j}}$ and $\boldsymbol{G_{i,j-\frac{1}{2}}}$ are computed analogically from the values $\boldsymbol{Q}_{i-1,j}^n$ and $\boldsymbol{Q}_{i,j}^n$ for the flux $\boldsymbol{F_{i-\frac{1}{2},j}}$ and $\boldsymbol{Q}_{i,j-1}^n$ together with $\boldsymbol{Q}_{i,j}^n$ for the flux $\boldsymbol{G_{i,j-\frac{1}{2}}}$.

The mesh widths Δx and Δy are given as

$$\Delta x = \frac{|I_1|}{N_x} \quad \text{and} \quad \Delta y = \frac{|I_2|}{N_y}.$$

The time step once again has to respect CFL condition, which in the two-dimensional case (2.6) has form

$$\Delta t = C_{CFL}\left(\frac{\bar{\lambda}_x}{\Delta x} + \frac{\bar{\lambda}_y}{\Delta y}\right)^{-1},$$

where

$$\bar{\lambda_x} = \max_{i,j} \lambda_x(\boldsymbol{Q}_{i,j})$$
$$\bar{\lambda_y} = \max_{i,j} \lambda_y(\boldsymbol{Q}_{i,j}).$$

The values of $\bar{\lambda_x}$ and $\bar{\lambda_y}$ are defined this way to ensure, that we will choose the time step, which makes the algorithm stable across the whole domain, not only locally. We are basically picking from the sequence of time step sizes the minimum value, which will satisfy the stability requirement for the whole mesh. After each time step, we have to compute a new size for the following one, since the variable and thus the eigenvalues are changed at each step.

The boundary can be treated the same way as in one-dimension using ghost cells, meaning if assume the domain $\boldsymbol{D}$ being surrounded by free boundaries, our conditions would for the x direction (flux $\boldsymbol{F}$) look like

$$\boldsymbol{Q}^n_{0,j} = \boldsymbol{Q}^n_{1,j}, \quad \boldsymbol{Q}^n_{N_x+1,j} = \boldsymbol{Q}^n_{N_x,j}$$

and for y direction (flux $\boldsymbol{G}$) then

$$\boldsymbol{Q}^n_{i,0} = \boldsymbol{Q}^n_{i,1}, \quad \boldsymbol{Q}^n_{i,N_y+1} = \boldsymbol{Q}^n_{i,N_y}.$$

If we wanted some boundary to be reflective, we would have to in addition reverse the sign of that velocity component, which is perpendicular to it, like it was shown in the one-dimensional case.

5.5. Source Terms

For fulfilling the goals of this thesis (namely the incorporation of wind) and forming a basis for possible future extension of this work, we will need to work with source terms in the numerical scheme. We will look at the idea of dealing with the source terms based on [16].

Let us assume, we have a general initial value problem for the non-homogeneous and non-linear system

$$\begin{aligned} \text{PDEs}: \quad & \frac{\partial \boldsymbol{q}}{\partial t} + \frac{\partial \boldsymbol{F}(\boldsymbol{q})}{\partial x} = \boldsymbol{S}(\boldsymbol{q}) \\ \text{IC}: \quad & \boldsymbol{q}(x, t_n) = \boldsymbol{q}_n, \end{aligned} \tag{5.19}$$

where $\boldsymbol{q}$ is the vector of unknowns, $\boldsymbol{F}(\boldsymbol{q})$ is the vector of fluxes and $\boldsymbol{S}(\boldsymbol{q})$ is the source term, which is some algebraic function of $\boldsymbol{q}$ and some other physical parameters. To develop a numerical scheme incorporating this term, we will need to make an assumption of no spatial variations in (5.19) , which simplifies to

$$\frac{\mathrm{d}\boldsymbol{q}}{\mathrm{d}t} = \boldsymbol{S}(\boldsymbol{q})$$

which is a system of ODEs.

Considering (5.19), we would like to compute $\boldsymbol{q}_{n+1}$ at time t_{n+1} from the value $\boldsymbol{q}_n$ at t_n. By splitting this problem, we obtain two initial value problems. The first one is

$$\begin{aligned} \text{PDEs :} \quad & \frac{\partial \boldsymbol{q}}{\partial t} + \frac{\partial \boldsymbol{F}(\boldsymbol{q})}{\partial x} = 0 \\ \text{IC :} \quad & \boldsymbol{q}(x, t_n) = \boldsymbol{q}_n \end{aligned} \tag{5.20}$$

and the second

$$\begin{aligned} \text{ODEs :} \quad & \frac{\mathrm{d}\boldsymbol{q}}{\mathrm{d}t} = \boldsymbol{S}(\boldsymbol{q}) \\ \text{IC :} \quad & \boldsymbol{Q}^{adv}, \end{aligned} \tag{5.21}$$

where the solution of (5.20) is $\boldsymbol{Q}^{adv}$, regarded as a predicted solution. This solution $\boldsymbol{Q}^{adv}$ then serves as an initial condition of the system (5.21), which is solved by a time $\Delta t = t_{n+1} - t_n$ and the solution $\boldsymbol{Q}_{n+1}$ is obtained, which is an approximation to the solution of (5.19). The initial condition $\boldsymbol{q}_n$ in (5.20) is the initial condition of the original problem (5.19).

We can define the *advection operator* $\mathcal{A}(\boldsymbol{q})$ and the *source operator* $\mathcal{S}(\boldsymbol{q})$ as follows:

$$\mathcal{A}: \quad \boldsymbol{Q}_i^{adv} = \boldsymbol{Q}_i^n - \frac{\Delta t}{\Delta x}[\boldsymbol{F}_{i+\frac{1}{2}} - \boldsymbol{F}_{i-\frac{1}{2}}]$$

and

$$\mathcal{S}: \quad \boldsymbol{Q}_i^{n+1} = \boldsymbol{Q}_i^{adv} + \Delta t\, \boldsymbol{S}(\boldsymbol{Q}_{\boldsymbol{i}}^{(\boldsymbol{s})}),$$

where $\boldsymbol{Q}_{\boldsymbol{i}}^{(\boldsymbol{s})}$ is the value at which the source term vector $\boldsymbol{S}$ is evaluated.

Then it can be written

$$\boldsymbol{Q}_i^{n+1} = \mathcal{S} \circ \mathcal{A},$$

which can be expressed as

$$\boldsymbol{Q}_i^{n+1} = \boldsymbol{Q}_i^n - \frac{\Delta t}{\Delta x}[\boldsymbol{F}_{i+\frac{1}{2}} - \boldsymbol{F}_{i-\frac{1}{2}}] + \Delta t\, \boldsymbol{S}(\boldsymbol{Q}_{\boldsymbol{i}}^{(\boldsymbol{s})}). \tag{5.22}$$

The choice for the term $\boldsymbol{Q}_{\boldsymbol{i}}^{(\boldsymbol{s})}$ can be written as a linear combination

$$\boldsymbol{Q}_{\boldsymbol{i}}^{(\boldsymbol{s})} = (1-\beta)\boldsymbol{Q}_i^n + \beta \boldsymbol{Q}_i^{adv} \tag{5.23}$$

and by setting $\beta = 0$ in (5.23), the scheme (5.22) will become

$$\boldsymbol{Q}_i^{n+1} = \boldsymbol{Q}_i^n - \frac{\Delta t}{\Delta x}[\boldsymbol{F}_{i+\frac{1}{2}} - \boldsymbol{F}_{i-\frac{1}{2}}] + \Delta t\, \boldsymbol{S}(\boldsymbol{Q}_{\boldsymbol{i}}^{\boldsymbol{n}}).$$

The same result can be also found in [13], where the authors present the formula for unstructured meshes.

In our case of two-dimensional Shallow water equations solved on structured grid mesh, the formula takes form

$$\boldsymbol{Q}_{i,j}^{n+1} = \boldsymbol{Q}_{i,j}^n - \frac{\Delta t}{\Delta x}[\boldsymbol{F}_{i+\frac{1}{2},j} - \boldsymbol{F}_{i-\frac{1}{2},j}] - \frac{\Delta t}{\Delta y}[\boldsymbol{G}_{i,j+\frac{1}{2}} - \boldsymbol{G}_{i,j-\frac{1}{2}}] + \Delta t\, \boldsymbol{S}. \tag{5.24}$$

6. Testing of the Model

In this chapter, we will present and discuss some test cases implemented in the *MATLAB* application *SWE2D*, which was programmed as a part of this thesis.

In the first section, we will describe the considered model more closely. In the second section, we introduce an addition of the wind source term. In the third section, we will look at the considered cases with graphical representation of the results. The fourth section serves to discuss the obtained results. The last section touches the subject of accuracy of the used numerical algorithm.

6.1. Description of the Model

The study of the coastal waves has to be done case by case, considering the unique geography of the domain, the flows properties there and choosing, what can be neglected and what cannot in that particular problem. Since any model of ocean waves, even under major simplifications, is not an easy task to do, we chose for the purpose of this master's thesis a couple of simple cases.

The program *SWE2D* solves numerically (see 5.4.2) the two-dimensional Shallow water equations in a rectangular domain $D = I_1 \times I_2$ bounded by Γ_s and Γ_c, where Γ_s signifies the boundary in sea and Γ_c is the boundary given by the profile of the coast, which we assume for simplicity to be composed of straight lines without any obstacles. The boundary Γ_s is assumed to be free and Γ_c to be reflective.

The interval $I_1 = [0, 2]$ will be partitioned into N_x elements and the interval $I_2 = [0, 1]$ into N_y elements. The gravitational acceleration is assumed $g = 9.812\, ms^{-2}$. The graphical representation will describe the situation at final time t. The constant for CFL condition is $C_{CFL} = 0.9$.

Except for the wind, we neglect the effect of any source terms like the bottom slope, bed friction, Coriolis force, rain, etc... These effects will be discussed in the chapter 7 as possible extensions to the work, since they are beyond the scope of this master's thesis.

The outline of the situation can be seen in fig. 6.1.

6.2. Wind Source Term

The incorporation of source terms into the numerical scheme was covered in (5.5) in general. We will now focus on the wind effect specifically.

As stated in [10], the effect of wind can be included to the equations as

$$\boldsymbol{S} = \begin{bmatrix} s_1 \\ s_2 \\ s_3 \end{bmatrix} = \begin{bmatrix} 0 \\ c_f' w^2 \, cos\alpha \\ c_f' w^2 \, sin\alpha \end{bmatrix}, \tag{6.1}$$

where c_f' is the wind friction coefficient, w is the wind speed and α is the wind direction with respect to x-axis. The suggested values of the friction coefficient can be found in [17] for different speeds of wind. We will use the value $c_f' = 0.00114$, which is valid for the wind velocity $3\, ms^{-1} \leq w \leq 10\, ms^{-1}$.

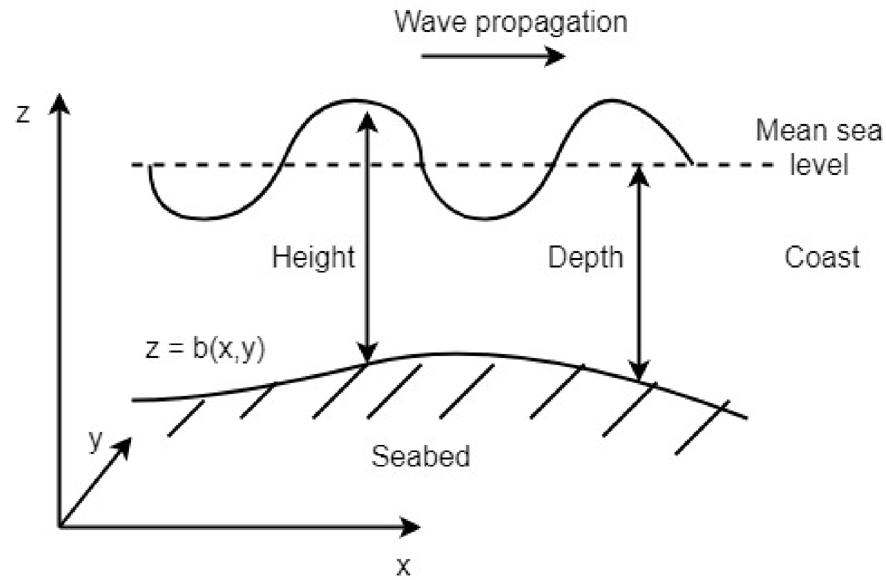

Figure 6.1: *Profile of the coastal area.*

Setting the value of w higher than $10\,ms^{-1}$ is not advised, since high speed velocities will cause the numerical scheme to become unstable. Also in such cases, the drag coefficient cannot be any longer considered to be a constant.

It has to be noted, that (6.1) is a very simplified approximation of the wind effect. With this approximation as a source term, we will now solve the system of the non-homogeneous two-dimensional Shallow water equations

$$\frac{\partial \boldsymbol{q}}{\partial t} + \frac{\partial \boldsymbol{F}}{\partial x} + \frac{\partial \boldsymbol{G}}{\partial y} = \boldsymbol{S},$$

where

$$\boldsymbol{q} = \begin{bmatrix} h \\ hu \\ hv \end{bmatrix}, \quad \boldsymbol{F} = \begin{bmatrix} hu \\ hu^2 + gh^2/2 \\ huv \end{bmatrix}, \quad \boldsymbol{G} = \begin{bmatrix} hv \\ huv \\ hv^2 + gh^2/2 \end{bmatrix}, \quad \boldsymbol{S} = \begin{bmatrix} 0 \\ c_f' w^2\, cos\alpha \\ c_f' w^2\, sin\alpha \end{bmatrix},$$

using the obtained numerical scheme (5.24) and using the Rusanov numerical flux as seen in (5.4.2).

6.3. Test Cases

6.3.1. Constant Initial Height, Flat Bottom, One Reflective Boundary

The first scenario (fig. 6.2) simulates an initially calm water surface, moving towards a solid wall over a flat bottom. Thus it follows a reflection creating a solitary wave.

The conditions of the experiment are following:

Initial height of surface $h_0 = 2\,m$, function of sea bed $b = 0$, wind speed $w = 10\,ms^{-1}$, direction of wind $\alpha = \pi$ (offshore) and one reflective boundary at $x = 2$. The initial velocities are $u_0 = 1\,ms^{-1}$ and $v_0 = 1\,ms^{-1}$. The resolution is $N_x = 300$ and $N_y = 100$. The time of observation is $t = 0.13\,s$. The total computational time was 2 minutes and 12 seconds.

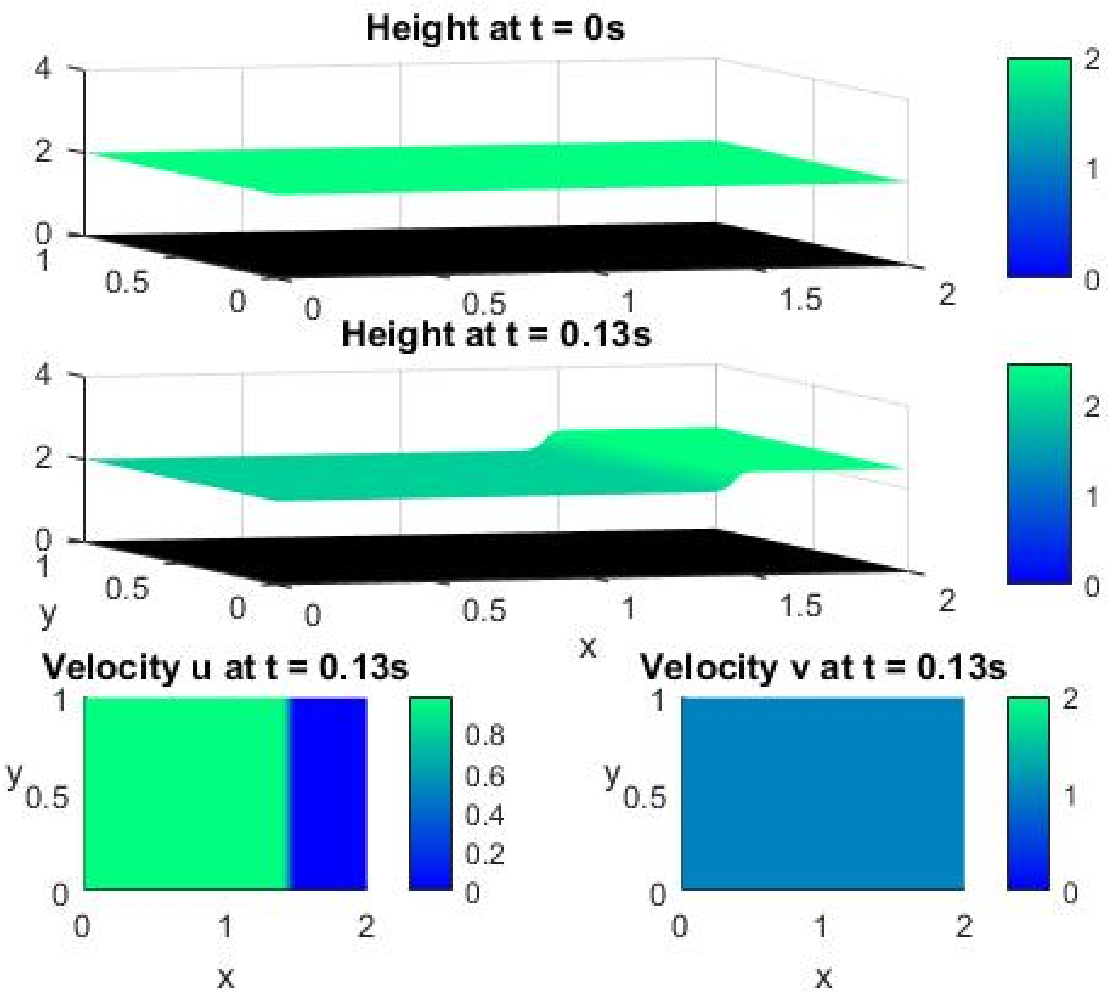

Figure 6.2: *Test case 1.*

6.3.2. Variable Initial Height, Flat Bottom Slope, One Reflective Boundary

The second scenario (fig. 6.3) is similar to the first one, except now the bottom is elevated, which could remind a situation, when the water approaches a shore.

The conditions of the experiment are following:

Initial height of surface $h_0(x) = 2 - b(x)\,m$, sea bed $b(x) = x\,tan(\pi/5)$, wind speed $w = 10\,ms^{-1}$, direction of wind $\alpha = \pi$ (offshore) and one reflective boundary at $x = 2$. The initial velocities are $u_0 = 1\,ms^{-1}$ and $v_0 = 1\,ms^{-1}$. The resolution is $N_x = 300$ and $N_y = 100$. The time of observation is $t = 0.13\,s$. The total computational time was 2 minutes and 10 seconds.

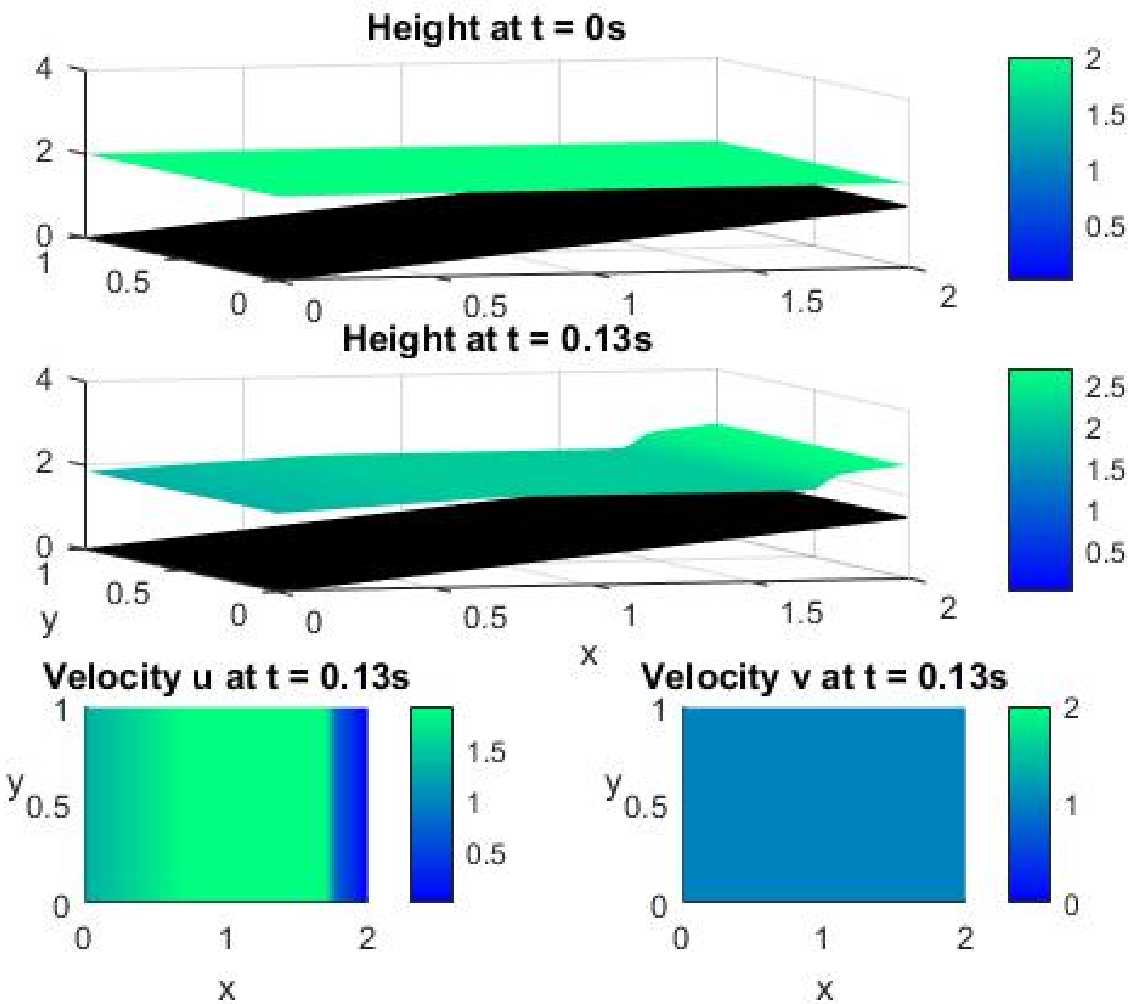

Figure 6.3: *Test case 2.*

6.3.3. Variable Initial Height, Flat Bottom Slope, Two Reflective Boundaries

The setting of the third test case (fig. 6.4) is identical to the previous one, except now we have two solid walls, so the situation may be interpreted as if the water approached a shore, which is also next to a steep cliff.

The conditions of the experiment are following:

Initial height of surface $h_0(x) = 2 - b(x)\,m$, sea bed $b(x) = x\,tan(\pi/5)$, wind speed $w = 10\,ms^{-1}$, direction of wind $\alpha = \pi$ (offshore) and two reflective boundaries. One at $x = 2$ and the second at $y = 1$. The initial velocities are $u_0 = 1\,ms^{-1}$ and $v_0 = 1\,ms^{-1}$. The resolution is $N_x = 200$ and $N_y = 200$. The time of observation is $t = 0.13\,s$. The total computational time was 3 minutes and 30 seconds.

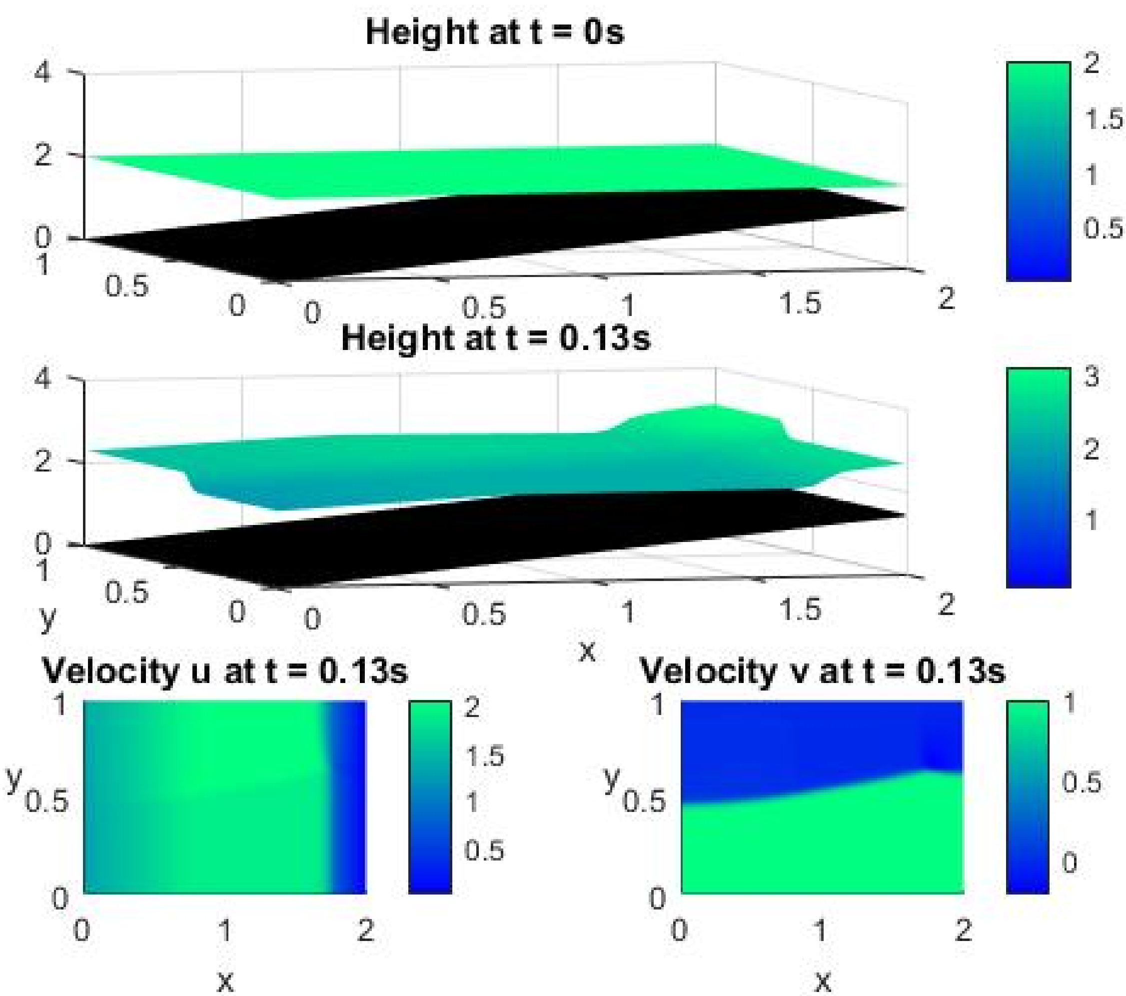

Figure 6.4: *Test case 3.*

6.3.4. Sinusoidal Initial Height, Flat Bottom Slope, One Reflective Boundary

The fourth scenario (fig. 6.5) is similar in its setting to the test case two, but now we no longer assume the water surface is initially calm, but rather assumes a sinusoidal pattern.

The conditions of the experiment are following:

Initial height of surface $h_0 = 2 + 0.5\, sin(12x) - b(x)\, m$, sea bed $b(x) = x\, tan(\pi/7)$, wind speed $w = 10\, ms^{-1}$, direction of wind $\alpha = \pi$ (offshore) and one reflective boundary at $x = 2$. The initial velocities are $u_0 = 1\, ms^{-1}$ and $v_0 = 1\, ms^{-1}$. The resolution is $N_x = 300$ and $N_y = 100$. The time of observation is $t = 0.13\, s$. The total computational time was 2 minutes and 17 seconds.

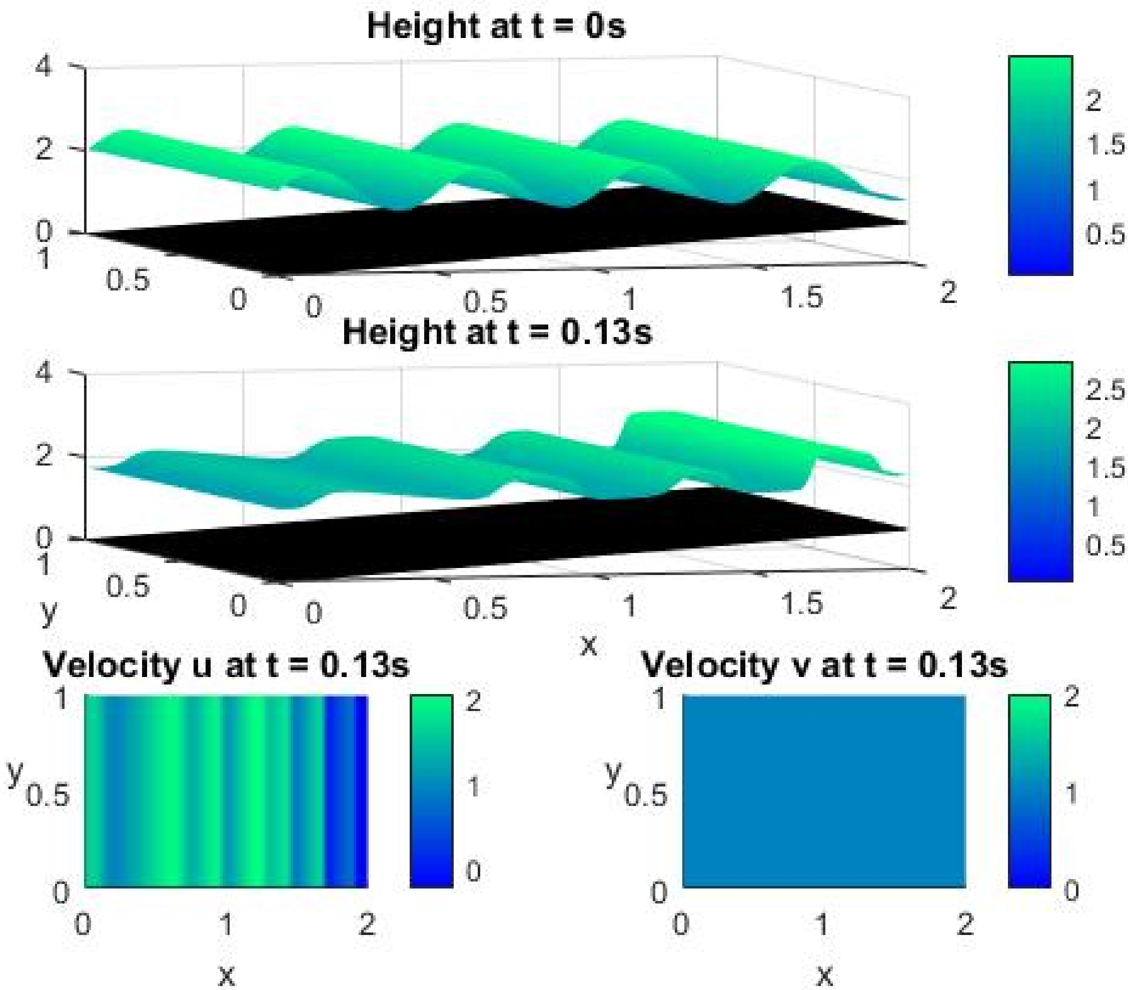

Figure 6.5: *Test case 4.*

6.3.5. Sinusoidal Initial Height, Sinusoidal Bottom Slope, One Reflective Boundary

The fifth test case (fig. 6.6) resembles the previous fourth case, but we suppose now, that the initially disturbed water approaches a shore over an uneven sea bed.

The conditions of the experiment are following:

Initial height of surface $h_0 = 2 + 0.5\,sin(12x) - b(x)\,m$, sea bed $b(x) = 0.5x + 0.25\,e^{-0.5x}\,sin(8x)$, wind speed $w = 10\,ms^{-1}$, direction of wind $\alpha = \pi$ (offshore) and one reflective boundary at $x = 2$. The initial velocities are $u_0 = 1\,ms^{-1}$ and $v_0 = 1\,ms^{-1}$. The resolution is $N_x = 300$ and $N_y = 100$. The time of observation is $t = 0.13\,s$. The total computational time was 2 minutes and 19 seconds.

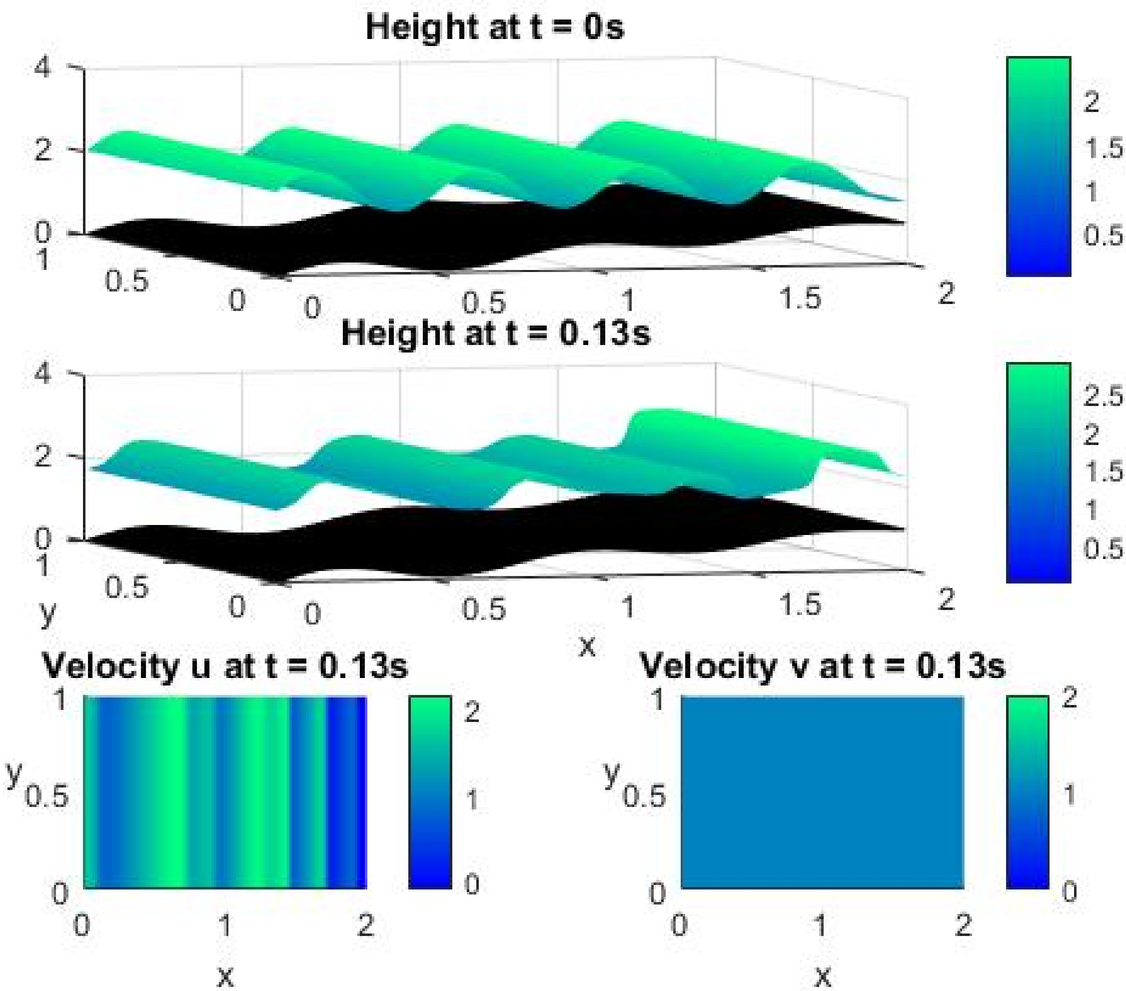

Figure 6.6: *Test case 5.*

6.3.6. Sinusoidal Initial Height, Sinusoidal Bottom Slope, Two Reflective Boundaries

The sixth scenario (fig. 6.7) is the last one dealing with near-shore areas. It is a combination of all the previous ones, where we suppose, that the initially disturbed water approaches a shore over an uneven sea bed and the shore is neighbouring with a steep cliff, which creates the second solid boundary.

The conditions of the experiment are following:

Initial height of surface $h_0 = 2 + 0.5\,sin(12x) - b(x)\,m$, sea bed $b(x) = 0.5x + 0.25\,e^{-0.5x}\,sin(8x)$, wind speed $w = 10\,ms^{-1}$, direction of wind $\alpha = \pi$ (offshore) and two reflective boundaries. One at $x = 2$ and the second at $y = 1$. The initial velocities are $u_0 = 1\,ms^{-1}$ and $v_0 = 1\,ms^{-1}$. The resolution is $N_x = 300$ and $N_y = 200$. The time of observation is $t = 0.13\,s$. The total computational time was 6 minutes and 25 seconds.

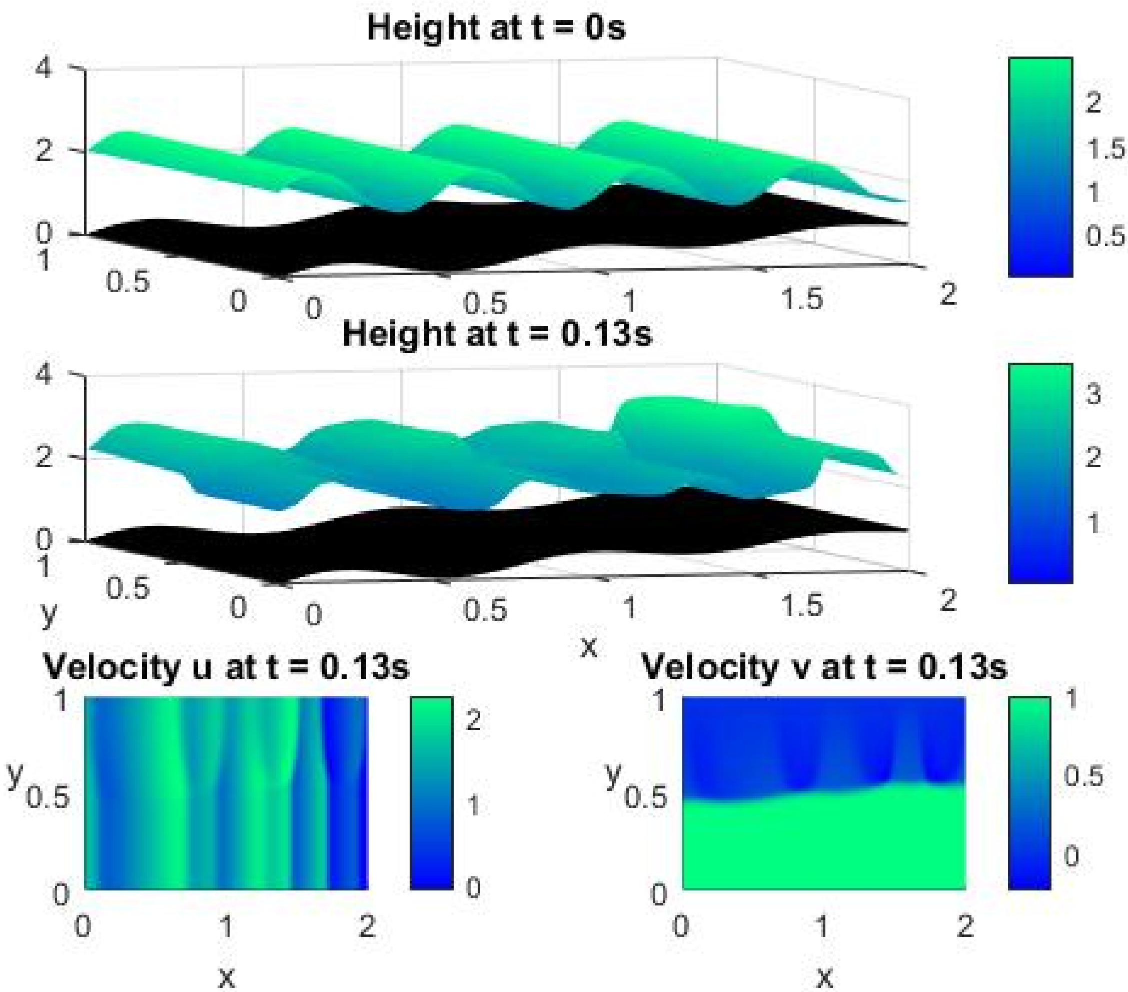

Figure 6.7: *Test case 6.*

6.3.7. Dambreak

The last case(fig. 6.8) simulates a dambreak. It is one of the typical scenarios, when it comes to modelling of water waves. The initial height of surface is

$$h_0 = \begin{cases} 2\,m & \text{if } x < (y-0.5)^2 + 0.75 \\ 1.5\,m & \text{otherwise} \end{cases}.$$

The sea bed is $b(x) = 0$, and wind speed is $w = 0\,ms^{-1}$. All boundaries are assumed to be free. The initial velocities are $u_0 = 0\,ms^{-1}$ and $v_0 = 0\,ms^{-1}$. The resolution is $N_x = 300$ and $N_y = 300$. The time of observation is $t = 0.10\,s$. The total computational time was 7 minutes and 12 seconds.

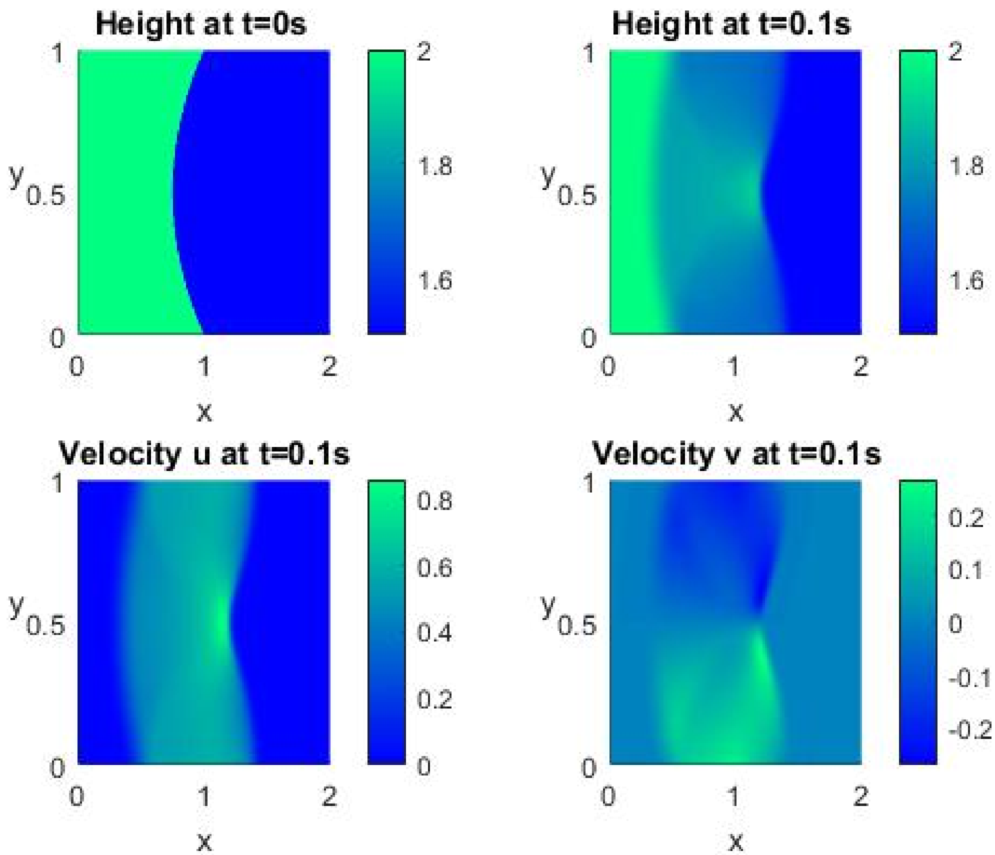

Figure 6.8: *Test case 7.*

6.4. Discussion of the Test Cases

Due to the computational time required for large areas with a fine mesh, only small domains were chosen. For a simulation of flow in more realistic domains, parallel and object-oriented programming would be required. Let us make three observations about the results.

The first one is, that the velocity v remains unchanged in the test cases 1,2,4 and 5. This is due to the fact, that the reflective barriers in these cases were parallel to its direction. The wave propagated in the direction of v, however since the boundaries perpendicular to it were free, there was nothing, what could influence the velocity v. If we look on the other hand on the cases 3,6 and 7, where there was some obstacle for the v-direction of the wave propagation, the velocity v changes with time and makes the wave profile asymmetrical (except for the case 7 due to the unique geometry).

The second remark is concerning the wind. As the reader can observe, there is no comparison of the same case with different speed velocities. That's because, if we have done so, the two images of situations with $w = 10\,ms^{-1}$ and $w = 0\,ms^{-1}$ would have looked absolutely identical on the paper. We noticed, that the used approximation 6.1 doesn't noticeably contribute to the wave propagation. The results are of course different, but the change in height for the two cases is in $\mathcal{O}(10^{-3})$. Based on these results, we have to state, that the effect of the shape of sea bed is in our model much greater in the near-shore areas, than the effect of wind, which is negligible. However, as we already stated, the used approximation (6.1) is quite simplistic, thus another, more precise, wind approximation would be needed to support or challenge this observation.

The third observation is, that our model successfully captures the reflection (2.4.5) of the waves. However, since we have used a rectangular mesh, the used numerical algorithm doesn't include a normal vector, which would bind the velocity components together and thus the reflection can be observed only, when the wave moves perpendicularly to the reflective barrier.

6.5. Accuracy

We wanted to measure, how close are the obtained results to the exact solution or at least have some idea, if the algorithm is convergent. For this purpose, we have chosen to study more closely the fifth test case (6.3.5). We kept the conditions exactly as they were (along with the time of observation), except for the discretization of the domain. We studied the solution, as we refined the mesh, by decreasing the mesh size in the x-direction. That is because the x-direction is in this case a characteristic propagation direction (due to the reflective barrier, which will affect the velocity u) of the wave approaching the shore, so we expect the main dependency of accuracy of the solution on the value of N_x. The number of partitions of the interval I_2 was always set to $N_y = 50$, in order to reduce the computational time to a reasonable value.

Of course, we don't have the exact solution, to which we could compare the approximated values of variables. For that reason, we have chosen as a reference state $\boldsymbol{q}$ the solution, when $N_x = 3200$. We have computed several approximated solution $\tilde{\boldsymbol{q}}$ for different values of N_x, starting at $N_x = 100$ and then doubling it up to $N_x = 1600$.

We then computed the relative errors as

$$err = \frac{\|\tilde{\boldsymbol{q}} - \boldsymbol{q}\|_\infty}{\|\boldsymbol{q}\|_\infty},$$

where $\|\|_\infty$ denotes the *infinity-norm.*

Remark. The *infinity-norm* $\|\boldsymbol{x}\|_\infty$ of a vector $\boldsymbol{x}$ is $\|\boldsymbol{x}\|_\infty = \max_{1\le i\le n} |x_i|$. Meaning, it is the absolute value of the largest component.

When computing the relative error, only values of $\boldsymbol{q}$ at grid nodes, where the approximate solution $\tilde{\boldsymbol{q}}$ is defined, are considered.

N_x	Relative error of $\tilde{\boldsymbol{q}}$
100	0.3258
200	0.2941
400	0.3148
800	0.2094
1600	0.1441

As we can observe fro the results, the relative errors are decreasing as we gradually refine the mesh in x direction. The only exception is the value of error for $N_x = 400$. But since the other values are in a decreasing sequence, we will assume, that this specific value may be inaccurate due to the nature of thus testing, where we refined only the x-direction as a significant one and neglected the y-direction, even though it has also impact on the solution. Or there might have been some "jump" in computing the state variables, which could have caused the relative error to spike.

This experiment leads us to belief, that the implemented algorithm is convergent to the exact solution.

7. Possible Extensions of the Work

In this chapter, we would like to propose, how the work could be built upon in the future.

The first section is a list of possible source term, that could be added into the existing model. The second section proposes other more general changes to the modelling structure.

7.1. Source Terms of Shallow Water Equations

Let us recall the Shallow water equations

$$\frac{\partial \boldsymbol{q}}{\partial t} + \frac{\partial \boldsymbol{F}}{\partial x} + \frac{\partial \boldsymbol{G}}{\partial y} = \boldsymbol{S},$$

where

$$\boldsymbol{q} = \begin{bmatrix} h \\ hu \\ hv \end{bmatrix}, \quad \boldsymbol{F} = \begin{bmatrix} hu \\ hu^2 + gh^2/2 \\ huv \end{bmatrix}, \quad \boldsymbol{G} = \begin{bmatrix} hv \\ huv \\ hv^2 + gh^2/2 \end{bmatrix}, \quad \boldsymbol{S} = \begin{bmatrix} s_1 \\ s_2 \\ s_3 \end{bmatrix},$$

where the vector $\boldsymbol{S}$ represents the source terms. For the purposes of this thesis, we have assumed, that this vector was a zero vector for the most part of the work and only assumed a wind source term later on for the numerical solution. Let's have a look, how would the equation have changed, if we had assumed its dependency on certain additional effects. These terms would have to be discretized in order to be included to the numerical algorithm.

7.1.1. Bottom Topography

We have already encountered this effect, when deriving the shallow water equations (4.1). In case of considering the effect of bottom slope, the source term would have taken the form

$$\boldsymbol{S} = \begin{bmatrix} s_1 \\ s_2 \\ s_3 \end{bmatrix} = \begin{bmatrix} 0 \\ -gh\frac{\partial}{\partial x}d \\ -gh\frac{\partial}{\partial y}d \end{bmatrix}.$$

7.1.2. Bed friction

Important factor in real flows is the bed friction, caused by the bed roughness. There are usually two formulations for this term. The first comes from Chezy (1769) and the other later on from Manning (1889). We will present here the latter and in such case the source term is

$$\boldsymbol{S} = \begin{bmatrix} s_1 \\ s_2 \\ s_3 \end{bmatrix} = \begin{bmatrix} 0 \\ -\tau_f^x \\ -\tau_f^y \end{bmatrix}.$$

Manning proposed following computation of the bed shear stress:

$$\tau_f^x = C_f u \sqrt{u^2}$$
$$\tau_f^y = C_f v \sqrt{v^2}$$

The coefficient C_f is the *Manning's bed friction coefficient*. It is computed from

$$C_f = g\frac{n^2}{\sqrt[3]{h}},$$

where n is the *Manning's bed roughness factor*. Chow (1959) created a table, where the values of n are proposed for many types of flow. As stated in [1], a typical value for C_f is 0.015.

7.1.3. Coriolis Force

The *Coriolis force* is an apparent force caused by the Earth's rotation and is responsible for the deflection of (for example) winds, airplanes and ocean currents towards east in the northern hemisphere and towards west in the southern hemisphere.

The source term including the Coriolis force takes form as presented in [6]

$$\boldsymbol{S} = \begin{bmatrix} s_1 \\ s_2 \\ s_3 \end{bmatrix} = \begin{bmatrix} 0 \\ -fhv \\ fhu \end{bmatrix},$$

where f is the *Coriolis parameter* given by

$$f = 2\Omega\, sin\phi,$$

The angular velocity of Earth is denoted by Ω and ϕ is the latitude.

Remark. The *latitude* of a given point on the Earth's surface is defined as the angle that a straight line, passing through this point and the center of Earth, subtends with respect to the equatorial plane

7.1.4. Wind

The used approximation (6.1) was quite simple and had little impact on the solution. Thus one of the possible modifications to the work might be an usage of another implementation for the wind.

7.2. Other Possible Modifications

Other possible extensions of the work may include a change in the numerical solution of the Shallow water equations. Not only the implementation of the Finite element or the Finite difference methods, but also a change of the numerical flux. For example using Roe's scheme or Steger-Warming's scheme and then compare the efficiency of the different numerical solutions. An important aspect of the numerical schemes is the generation of mesh. For simplicity of our domain, we chose the rectangular mesh, which would perform poorly given more irregular boundaries. Thus the implementation of a triangular mesh on more complex domain is suggested.

Another, more drastic suggestion, is to base the model on different governing equations. As already mentioned in the chapter 3, we considered beside theShallow water equations also the Mild-slope equation and the Boussinesq equations. Those are of course not the only options by far. One may attempt to model ocean waves by more sophisticated means of spectral wave models for instance.

8. Conclusion

This master's thesis was focused on a study of the motion of ocean waves. Several different equations and numerical methods were considered as possibilities for the modelling. The main focus of this work in on the derivation, analysis and numerical solution of the Shallow water equations by the Finite volume method. The resulting numerical scheme includes a shape of the sea bed and a wind as influencing factors of the solution.

The contribution of this work lies in the proof, that the studied system of equations are hyperbolic and based on this result, an appropriate numerical method was chosen. Next contribution is the proposition of a numerical algorithm, using the Rusanov numerical flux, for the solution of the two-dimensional Shallow water equations. An important addition, compared to the most of the other basic solvers available, is the wind velocity and direction, since the effect of wind is often completely neglected. The obtained results displayed a principal fact, that the inclusion of wind had little impact on the solution. This may be due to the usage of a too simplistic wind approximation, which isn't capable sufficiently model its effect. However based on the results, we had to state, that in near-shore areas, which were considered as test cases, the shape of bed had a dominant influence on the computation, using the proposed numerical algorithm. The proposed numerical scheme was implemented in the environment of MATLAB. The thesis contains the achieved graphical results of several test cases done in *SWE2D*, which are then discussed. The accuracy of the numerical algorithm was then tested on a chosen test case and we find the approximate solutions to be convergent to the exact one.

The goal of this thesis was to formulate a model of surface water waves, which takes into consideration a wind speed and a shape of sea bed and implement it in MATLAB. This goal was achieved, however, due to the complexity of the task, which is the modelling of ocean waves, the author recognizes, that this work serves as an initial step for a modelling in the realistic conditions, which is beyond a scope of a master's thesis. One model cannot generalize the very specific environment of each considered domain. For that reason, several possible extensions of the work were proposed in the thesis. Namely an incorporation of a different approximation of a wind in order to compare the achieved results and discuss them. Another suggestion is an addition of other important source terms like a bed friction and the Coriolis force and formulating the numerical solution for triangular meshes, which would be needed for discretizing more complex domains. Also the author advices, for a future implementation, the usage of parallel and object-oriented programming to achieve better computational times.

Bibliography

[1] BAINES, P. G.: On the drag coefficient over shallow water. *Boundary-layer meteorology*, vol 6, 1974, p. 299-303.

[2] BERKHOFF, J. C. W.: *Mathematical Models for Simple Harmonic Liner Water Waves-wave Diffraction and Refraction*. [PhD Thesis.] The Netherlands: Delft Hydraulic Lab., 1976. 103 p.

[3] BOOIJ, N.: A note on the accuracy of the mild-slope equation. *Coastal Engineering*, vol 7, 1983, p. 191-203.

[4] ÇENGEL, Y. A. and CIMBALA, J. M.: *Fluid mechanics : fundamentals and applications*. McGraw-Hill, 2006, 929 p. ISBN 0–07–247236–7

[5] CERMAK, L.: *Matematické metody v teorii proudění*. [elektronická skripta], 2016, 90 s. Dostupné z: http://math.fme.vutbr.cz/cz/?staff=s_%C4%8Derm%C3%A1k

[6] CHERTOCK, A., DUDZINSKI, M., KURGANOV, A. and LUKAČOVÁ-MEDVIĎOVÁ, M.:Well-balanced schemes for the shallow water equations with Coriolis forces. *Numerische Mathematik*, vol 138, 2017, p. 939-973.

[7] FRANCŮ, J.: *Parciální diferenciální rovnice*. Akademické nakladatelství CERM, s.r.o. Brno, 2011, 160 s. ISBN 978-80-214-4399-0

[8] HALLIDAY, D., RESNICK, R. and WALKER J.: *Fyzika*. Vysoké učení technické v Brně, nakladatelství VUTIUM, 2000, 1198 s. ISBN 80-214-1869-9

[9] HUNT, J. N.: *Gravity Waves in Water of Finite Depth*. Computational Mechanics Publications, Southampton, 1997, p. 169-213 ISBN 185312351X

[10] JHA, A.: *Object-Oriented Hyperbolic Solver on 2D-Unstructured Meshes Applied to the Shallow Water Equations*. [PhD Thesis.] Loughborough University, Department of Civil and Building Engineering, 2006. 274 p.

[11] LEVEQUE, R.: *Finite Volume Methods for Hyperbolic Problems.*. Cambridge University Press, 2003, 558 p. ISBN 0-511-04219-1

[12] NWONGU, O.: An alternative form of the Boussinesq equations for nearshore wave propagation. *Journal of Waterway, Port, Coastal, and Ocean Engineering, ASCE*, vol 119, 1993, p. 618-638.

[13] PAN, C., DAI S. and CHEN S.: Numerical simulation for 2D shallow water equations by using Godunov-type scheme with unstructured meshes. *Journal of Hydrodynamics*, vol 18, 2006, p. 475-480.

[14] PEREGRINE, D. H.: Long waves on a beach. *Journal of Fluid Mechanics*, vol 27, no. 4, 1967, p. 815-827.

[15] SORENSEN, R. M.: *Basic coastal engineering*. Springer Science Business Media, Inc., 2006, 324 p. ISBN: 0-387-23332-6

[16] TORO, E. F.: *Shock-Capturing Methods for Free-Surface Shallow Flows.* John Wiley & Sons, Inc., 2001, 309 p. ISBN 0-471-98766-2

[17] TRENBERTH, K. E., LARGE, W. G. and OLSON, J. G.: The effective drag coefficient for evaluating wind stress over the oceans. *American Meteorological Society*, vol 2, 1989, p. 1507-1516.

[18] YOUNG, I. R.: *Wind generated ocean waves.* Elsevier ocean engineering book series; v.2, 1999, 288 p. ISBN 0-08-043317-0

[19] WEI, G., KIRBY J. T. and STEPHAN T. G.: A fully nonlinear Boussinesq model for surface waves. *Journal of Fluid Mechanics*, vol 294, 1995, p. 71-92.

9. Used Notations

t [$\mathtt{s}$]	time
g [$\mathtt{ms}^{-2}$]	gravitational acceleration
ρ [$\mathtt{kgm}^{-3}$]	density
ϕ [$\mathtt{m}^2\mathtt{s}^{-1}$]	velocity potential
u [$\mathtt{ms}^{-1}$]	x-axis component of the velocity
v [$\mathtt{ms}^{-1}$]	y-axis component of the velocity
w [$\mathtt{ms}^{-1}$]	z-axis component of the velocity
a [$\mathtt{m}$]	wave amplitude
H [$\mathtt{m}$]	wave height
L [$\mathtt{m}$]	wave wavelength
T [$\mathtt{s}$]	period
p [$\mathtt{kgm}^{-1}\mathtt{s}^{-2}$]	pressure
c [$\mathtt{ms}^{-1}$]	phase speed
k [$\mathtt{m}^{-1}$]	wave number
ω [$\mathtt{rads}^{-1}$]	angular velocity
d [$\mathtt{m}$]	depth
μ [$\mathtt{kgm}^{-1}\mathtt{s}^{-1}$]	dynamic viscosity
ν [$\mathtt{m}^2\mathtt{s}^{-1}$]	kinematic viscosity
h [$\mathtt{m}$]	total height of a water column
η [$\mathtt{m}$]	function of free surface
$\boldsymbol{q}$	vector of conserved variables
$\boldsymbol{F}$	flux in x-direction
$\boldsymbol{G}$	flux in y-direction
b	profile of a sea bed
λ	eigenvalue
C_{CFL}	constant for CFL condition
w [$\mathtt{ms}^{-1}$]	wind speed

$\boldsymbol{D}$	considered domain
I_1 [m]	length of domain in x-direction
I_2 [m]	length of domain in y-direction
N_x	number of partitions of I_1
N_y	number of partitions of I_2